Cholesterol contents in human macrophages regulate their inflammatory responses.

Dila Aycan

Thesis submitted to the University of Ottawa in partial Fulfillment of the requirements for the MSc degree in Biochemistry with specialization in Human and Molecular Genetics

Department of Biochemistry, Microbiology and Immunology

Faculty of Medicine

University of Ottawa

Abstract

Atherosclerosis is a chronic inflammatory and lipid disorder caused by the buildup of cholesterol-loaded cells of monocyte and muscle cell origin in the arterial intima. While the relationship between excess cholesterol and macrophage behavior is well observed, the molecular mechanisms linking the two remain unclear. Therefore, characterizing the pathways from changes in intracellular cholesterol to the resulting inflammatory output is key to understanding the behavioral changes observed in human macrophages *in vitro*. We identified that THP-1 macrophages acutely depleted of cholesterol increase the expression of JMJD3, an H3K27me3 demethylase. By using IL-10 as a marker for immune-modulating genes and TNF-α as a marker for pro-inflammatory genes, cholesterol-depleted THP-1 macrophages responded inconsistently to LPS and echinomycin, an inhibitor of HIF-1α, as determined by RT-qPCR and ELISA. Further studies investigating other regulators and outputs of macrophage behavior linked to cellular cholesterol modification are required.

Acknowledgements

“Science is the only true guide in life.”

M.K. Atatürk

I would like to recognize my wonderful family and partner for their consistent support and unconditional love. My mother’s stories of little soldiers fighting germs in our bodies generated so much interest in me as a 3-year old picky eater that I now present to you the collection of my knowledge of this soldier, the macrophage.

I send my sincerest gratuities to my thesis advisory committee members, Drs. Robin Parks and Alexander Sorisky, and thesis examination members, Drs. Mireille Ouimet and Morgan Fullerton, for their support and guidance as I learn and grow as a scientist. The enthusiasm and opportunities provided by Dr. Katey Rayner, whom I thank tremendously, during my most difficult days pushed me forward. I also extend my gratitude to Dr. Douglas Gray, who always encouraged my dreams and shared my love for genetics. Finally, I thank my research supervisor, Dr. Xiaohui Zha, for her support and extensive knowledge.

I thank my lab members Michelle Yuan and Dr. Zeina Salloum for providing technical training and being my friend. It was also a pleasure to pass on my gained knowledge to the newer lab members during the short time we worked together. I appreciate my friends, old and new, for supporting me in Ottawa.

It has been an honor and privilege to have studied at the University of Ottawa. Successfully finishing this chapter of my life fills me with determination.

Table of Contents

List of Abbreviations

Acetyl Co-A	Acetyl Coenzyme A
ABC	ATP Binding Cassette (Subfamily A/G Member 1)
AMPK	5' adenosine Monophosphate-Activated Protein Kinase
Apo	Apolipoprotein (AI, AII, B, E)
ATGL	Adipose Triglyceride Lipase
ATCC	American Type Culture Collection
ATP	Adenosine Triphosphate
AP-1	Activator Protein 1
BSA	Bovine Serum Albumin
BMDM	Bone Marrow-Derived Macrophage
cDNA	Complementary DNA
CD	Cluster of Differentiation (11b, 13, 36, 163, 206)
CGI-58	Comparative Gene Identification-58
CO_2	Carbon Dioxide
C_t	Cycle Threshold
DAMP	Damage Associated Molecular Pattern
dH_2O	Distilled Water
DNA	Deoxyribonucleic Acid
dNTP	Deoxynucleotide Triphosphates
DMEM	Dulbecco's Modified Eagle Medium
DMSO	Dimethyl Sulfoxide
ELISA	Enzyme-Linked Immunosorbent Assay
ER	Endoplasmic Reticulum
EZH2	Enhancer of Zeste Homolog 2
FBS	Fetal Bovine Serum
gDNA	Genomic Deoxyribonucleic Acid
H_2SO_4	Sulfuric Acid
H3K4me3	Trimethylation of Histone 3 Lysine 4
H3K27me3	Trimethylation of Histone 3 Lysine 27
HIF-1α	Hypoxia-Inducible Factor Type 1 alpha
HDAC	Histone Deacetylase (2, 9)
HDL	High-Density Lipoprotein
HMGCR	3-Hydroxy 3-Methylglutaryl Coenzyme A Reductase
HPRT1	Hypoxanthine Phosphoribosyltransferase 1
HRE	Hypoxia Response Element
HRP	Horseradish Peroxide
ICAM-1	Intracellular Adhesion Molecule 1
IL	Interleukin (1β, 6, 10, 18)
JARID1	Lysine Specific Demethylase 5b/Jumonji, AT rich Interactive Domain 1
JMJD3	Lysine Specific Demethylase 6b/Jumonji Domain Containing 3
KDM	Lysine Demethylase
LDL	Low-density Lipoprotein
LDL-C	Low-density Lipoprotein Cholesterol
LDLR	Low-density Lipoprotein Receptor

LPS	Lipopolysaccharide
LRP	Low-density Lipoprotein Receptor–Related Protein (1, 5)
LXR	Liver X Receptor
MCD	Methyl-β-Cyclodextrin
MCP-1	Monocyte Chemoattractant Protein 1
M-CSF	Macrophage Colony Stimulating Factor
miR-33	Micro Ribonucleic Acid-33
NADPH	Dihydronicotinamide-Adenine Dinucleotide Phosphate
NLRP3	NLR Family Pyrin Domain Containing 3
NF-κB	Nuclear Factor kappa-Light-Chain-Enhancer of Activated B Cells
NPC1L1	Niemann–Pick Type C1-Like 1
oxLDL	Oxidized Low-Density Lipoprotein
PCSK9	Proprotein Convertase Subtilisin/Kexin Type 9
PBS	Phosphate Buffered Saline
PK	Protein Kinase (A, C)
PMA	Phorbol 12-Myristate 13-Acetate
PPARγ	Peroxisome Proliferator-Activated Receptor Gamma
PRC2	Polycomb-Repressive Complex 2
PS	Penicillin-Streptomycin
RCF	Relative Centrifugal Force
ROS	Reactive Oxygen Species
RNA	Ribonucleic Acid
RNAse	Ribonuclease
RPMI	Roswell Park Memorial Institute (Medium)
RT-qPCR	Real-Time Quantitative Polymerase Chain Reaction
SR	Scavenger Receptor (A, A1, I)
SREBP	Sterol Regulatory Element Binding Protein
TLR	Toll-Like Receptor (2, 4)
TMB	3,3′,5,5′-Tetramethylbenzidine
TNF-α	Tumor Necrosis Factor-alpha
VCAM-1	Vascular Adhesion Molecule 1
VLDL	Very Low-Density Lipoprotein
VSMC	Vascular Smooth Muscle Cell

List of Figures

List of Tables

CHAPTER ONE: Introduction

1.1 Literary Background of Atherosclerosis

Cardiovascular diseases cost the Canadian government 21 billion dollars per year and the lives of a third of the Canadian population[1]. Atherosclerosis is a disease of multifactorial origins: a disease of exposure to genetic, lipid and immunological risk factors over decades, and is one of the primary causes of mortality worldwide[2–4]. Atherosclerosis is defined as the potentially life-threatening condition of the buildup of cholesterol-laden plaques in medium to large-sized arteries[3,5] and is a significant risk factor to the development of many cardiovascular diseases, such as myocardial infarction and unstable angina[4,6].

The complicated biological nature, high cost and worldwide prevalence of atherosclerosis require an intricate understanding of its development and molecular mechanisms. Ultimately, the development of targeted and personalized therapies for the reduction and idealistic elimination of atherosclerotic plaque size and severity is required for the minimization of its outcomes. Current treatments for atherosclerosis primarily consist of statins[7–9], the gold standard medication for lowering blood cholesterol by inhibiting *de novo* lipogenesis[7]. In addition, aspirin can also be utilized in the secondary prevention of atherosclerosis[8].

This project is dedicated to understanding the complex interplay between human macrophage cellular cholesterol contents and their inflammatory responses, which is hypothesized to be mediated through epigenetic signaling.

1.1.1 The role of macrophages in the pathogenesis of atherosclerosis

The arterial tunica intima is situated beneath the arterial endothelium and the tunica media, which contains VSMC[10]. Circulating LDL in the bloodstream may leak into the subendothelial space of the intima, and the risk factor of LDL leakage into the subendothelial space increases with high blood LDL concentration, especially since hypercholesterolemia is a significant risk factor for the development of atherosclerosis[11]. Additionally, dysfunction of the arterial endothelial layer due to factors such as turbulent flow, smoking or hypertension allows for increased permeability of the endothelium and the subsequent increase in LDL uptake[12]. In the subendothelial space, LDL can be retained by proteoglycans and modified by methods including lipoprotein aggregation and oxidation[13], which induces the secretion of chemokines and adhesion molecules by irritated arterial endothelial cells for leukocyte recruitment[5,6].

Upon receiving the endothelial stress signals/adhesion molecules and molecular patterns like oxLDL (classified as DAMPs)[14,15], circulating monocytes infiltrate from the blood lumen into the subendothelial space, which can use the endothelial adhesion molecules MCP-1, ICAM-1 and VCAM-1 for attachment [6,10,16,17]. Triggered by factors such as M-CSF[6], the monocytes can then differentiate into macrophages for the required inflammatory response (Figure 1). The monocyte to macrophage differentiation process is mainly facilitated by the lineage determining transcription factors such as AP-1[18]. Tissue-resident macrophages develop in a separate lineage than circulating blood monocyte-derived macrophages, with the resident macrophages developing in the embryonic yolk sac instead of the bone

marrow and are therefore not derived from hematopoietic stem cells[19,20]. Nevertheless, the response to two different macrophage types is similar for clearance of the irritant, LDL presence in the intima, in a process of “sterile inflammation”[4,18,19,21–24]. This inflammatory response to sterile triggers includes releasing ROS, which inadvertently results in the oxidation of LDL in the subintimal space[15,25,26]. Furthermore, proteoglycans binding Apo-B secreted by monocyte-derived macrophages contribute to lipoprotein retention in an already established atherosclerotic lesion[6], promoting the advancement of atherosclerosis. The modified lipoprotein and cholesterol overloaded macrophages, and smooth muscle cells[22], are triggered to favor the pro-inflammatory state of inflammation[15,18].

Native LDL is internalized in macrophages by the LDLR, which feeds into a negative feedback loop to downregulate LDLR on the plasma membrane. In short, downregulation is stimulated by excess cholesterol and native LDL in the environment[13,27]. Facilitated by cytosolic PCSK9-LDLR interactions, the PCSK9-LDLR complex is then directed to lysosomes for degradation[13], which prevents the recycling of LDLR to the plasma membrane, ultimately preventing further cellular ingestion of native LDL[11].

Modified LDL particles, such as oxLDL, cannot be ingested through LDLR-mediated endocytosis because LDLR is downregulated by excess cholesterol[13]. In the presence of hyperlipidemic environments rich with oxLDL, macrophages instead ingest oxLDL and other modified LDL through scavenger receptors, primarily CD36[4] and receptors from the scavenger receptor family, such as SR-A and SR-I[21,26], and LRP family members such as LRP5 and LRP1[13]. While LDLR is downregulated by

excess LDL, scavenger receptors are not downregulated by oxLDL in the environment[24]. The constant presence on the plasma membrane allows for the unrestricted oxLDL intake into macrophages, and the subsequent increase in macrophage cellular cholesterol content triggers a shift in macrophage behavior to become more pro-inflammatory, which includes responses such as the release of ROS and the signaling the recruitment of more leukocytes to the atherosclerotic lesion site[28,29]. The primary scavenger receptor for oxLDL uptake[25], CD36 expression can be upregulated by the nuclear receptor transcription factor PPARγ, a master regulator of immune and lipid metabolism, adipogenesis and their homeostatic states[30,31]. PPARγ is also responsible for mediating cholesterol efflux through the regulation of ABCA1 (which is also influenced by CD36[25]) and LXR, and suppressing pro-inflammatory responses by inhibiting NF-κB-induced binding to inflammatory cytokine promoters, such as TNF-α[31].

As the atherosclerotic lesion continues to develop due to unresolved inflammation, macrophages and VSMCs continue to ingest more cholesterol than the capacity of cholesterol transported out of peripheral cells to HDL (reverse cholesterol transport), intracellular cholesterol metabolism, or deposits into lipid droplets. If the sterile inflammation does not resolve LDL presence in the intima and continues uncontrolled cholesterol uptake in macrophages and VSMCs, the atherosclerotic lesion grows and has a greater potential of becoming more unstable. Foam cells, termed for their foamy appearance when overloaded with membrane-bound lipid droplets[6,32], contribute towards a significant portion of the atherosclerotic plaque, which can remain growing undetected for decades. While monocyte-derived

macrophages significantly contribute to the foam cell population, VSMC-derived foam cells can make up at least over half of the foam cell population[29]. However, it is unclear where in the atherosclerotic plaque the distribution of these SMC or macrophage-originating foam cells are[21].

While atherosclerosis is mostly benign[6], which can even be in the form of intimal thickening in adults[10], lesions become hazardous due to factors such as increased lesion size, which can obstruct blood flow, or reduced plaque cap thickness, which can lead to thrombosis. ROS secretion also induces the release of matrix metalloproteinases, which physically weaken the fibrous cap and walls of the atherosclerotic plaque[33]. As the atherosclerotic plaque grows and protrudes into the lumen, blood flow can be restricted due to the arterial radius decreasing in size. The thickness of the connective tissue layer that covers the advanced atherosclerotic plaque is one of the determinants of plaque stability, and thin layer plaques with higher lipid pools have a higher risk of rupture[34]. In the case of rupture, they can lead to arterial thrombosis to cause ischemia, which can result in unstable angina, myocardial infarctions, strokes and/or peripheral vascular disease[6].

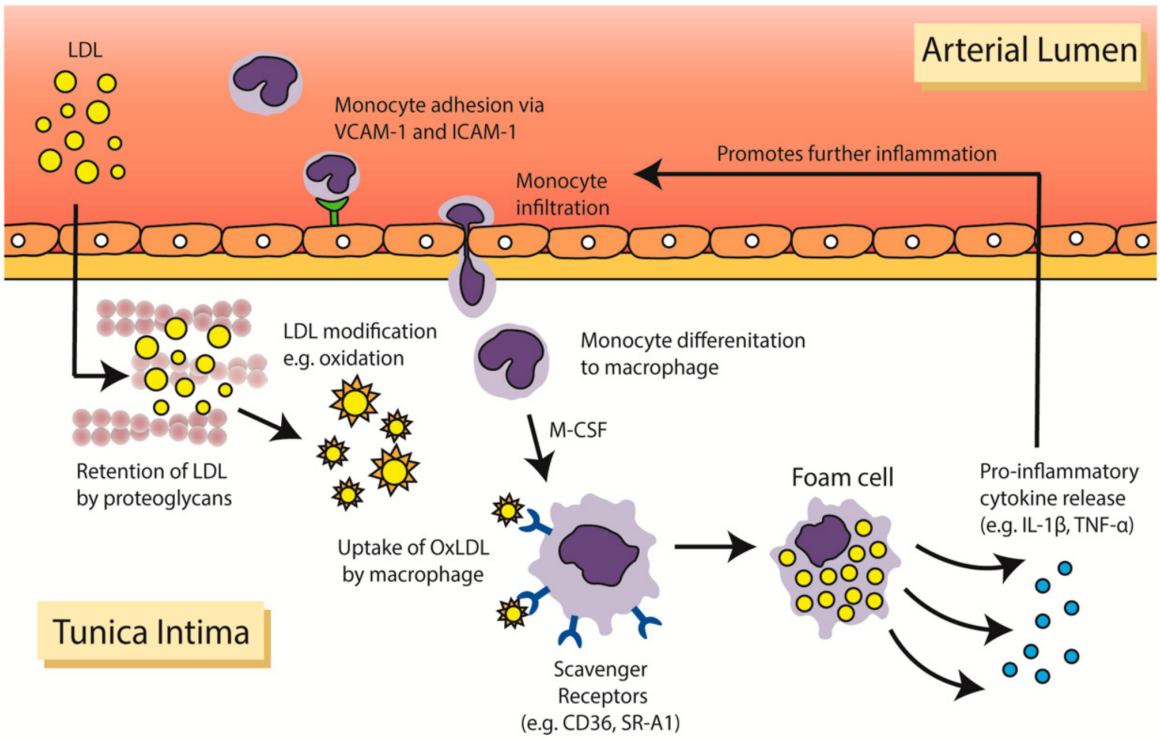

Figure 1. Infiltration of LDL and formation of macrophage foam cells in the arterial wall.
In individuals with hypercholesterolaemia, elevated levels of LDL-C are prone to infiltration and retention in the arterial wall. Monocytes recruited into the arterial wall differentiate into macrophages on stimulation by M-CSF. Modified LDL particles are then taken up by macrophages via scavenger receptors. Accumulation of lipids in the macrophage results in the formation of lipid-laden foam cells leading to the release of pro-inflammatory cytokines.

Figure and caption are taken from Nguyen MT, *et al.* 2019[35] under the terms and conditions of the Creative Commons Attribution (CC BY) license[36], Copyright © 2019 by the authors. Licensee MDPI, Basel, Switzerland[37]. Abbreviations and paragraph spacing were modified in this thesis for clarity.

1.2 Macrophages in Atherosclerosis

Described in the 19th century for their ability to phagocytose microbes[32], blood monocyte-derived macrophages are myeloid cells produced in the bone marrow[38] and are often the first responders to homeostatic disruptions and are involved in an array of bodily functions ranging from immune responses to tissue repair and development to the recruitment of adaptive immune cells lesion sites. Macrophages heavily contribute to the components of an atherosclerotic lesion, and therefore their behavior in atherosclerosis must be well understood for the development of treatment strategies and the establishment of novel molecular targets for cardiovascular disease therapy.

1.2.1. Macrophage phenotypic plasticity is a diverse spectrum

Depending on the inflammatory stimulus, macrophages can adopt extremely versatile phenotypes between the pro-inflammatory, “classically activated” (M1) and immune-modulating, “alternatively activated” (M2) macrophages[18,39] (Figure 2). The atherosclerotic plaque harbors macrophages that display extreme versatility and is heterozygous for the M1 and M2 phenotypes. Moreover, M2 macrophages are further subdivided into three categories: M2a, M2b, and M2c[39,40]. However, the M1 and M2 phenotypes describe extremes of the macrophage phenotypic plasticity spectrum and is not reflective of an absolute, categorical phenotype. In support of this statement, many macrophages display both M1 and M2 markers at the same time[41], and macrophages that exhibit behaviors that cannot be described by either the aforementioned M1 or M2 phenotypes have also been described[40]. Macrophage

phenotypic plasticity is even more complex *in vivo*: the atherosclerotic plaque is heterozygous for many types of macrophage polarizations, with each phenotype dependent on the stimulant and its subsequent inflammatory response. Despite this heterozygosity, most M1-like macrophages are hypothesized to be located towards the edges of the plaque, increasing the risk of plaque rupture[18].

1.2.2. The role of cholesterol in macrophagic trained immunity

Chromatin consists of DNA wrapped around a core of 8 histone proteins: pairs of the histones H2A, H2B, H3 and H4[20,42,43]. The protruding N terminal of these histones can be modified by methods such as methylation and acetylation to induce changes in the chromatin accessibility[20], controlling the transcription of genes in nearby regions of the modified histones. The exposure of innate immune cells to conditions such as oxLDL, even for a brief period, can cause a shift in their behavior, resulting in a conditioned response in the future, long after the initial stimulus is removed. This is termed “trained immunity”[44] and is significantly controlled by epigenetic factors.

In particular, H3K27me3, a region associated with transcriptional repression[20,45–47], and H3K4me3, a region associated with transcriptional accessibility[20,47], are two potential targets of cholesterol-mediated inflammatory response. Numerous regulators of these regions exist, where JMJD3 and JARID1, two histone demethylases that are members of the KDM family, remove H3K27me3 and H3K4me3 markers, respectively[20,45,48]. Both JMJD3 and JARID1 are dependent on the transcription factor HIF-1α for their expression, as HIF-1α binds to their HRE

to induce transcription[46,48]. oxLDL induces TLR4-dependent NF-κB activation, which can promote the transcription of target genes, such as the components of the NLRP3 inflammasome complex, which results in the production of proinflammatory cytokines like IL-1β[24].

JMJD3 is a regulator of inflammatory genes that relate to both the M2 and M1 phenotypes, and is more essential in the development of the M2 phenotype than M1 activation[20,45,49]. It is also known that MCD activates the M2-like macrophage phenotype, facilitated by ABCA1-mediated PKA activation[50]. Oversaturation of cholesterol suppresses PKA to promote the M1-like macrophage phenotype *in vitro*. When stimulated with LPS, cholesterol-depleted macrophages secreted more IL-10 and cholesterol-overloaded macrophages were shown to secrete more TNF-α[50]. Both IL-10 and TNF-α require LPS and therefore the LPS receptor, TLR4, for the facilitation of their expression and secretion[41].

In addition to the role of PKA stated above, PKA acting downstream of ABCA1 can phosphorylate NF-κB. NF-κB can then activate macrophagic trained immunity through HIF-1α[51,52], which can, in turn, increase JMJD3 expression[46] to induce the transcription of target genes such as IL-10 but inhibit the expression of other NF-κB target genes such as TNF-α. Additionally, PKA can directly interact with HIF-1α to induce its target gene expression[53].

1.2.3 THP-1 cells as a model to study human macrophage behavior

While primary human macrophages are an ideal model to study human macrophage behavior *in vitro*, this project presents the results generated from THP-1 cells, the first immortalized monocytic leukemia cell line, exclusively[54].

Originally taken from a one-year-old male infant with acute monocytic leukemia from Japan and first described in Tsuchiya et al.'s 1980 paper[54], THP-1 cells have become a reliable model for assessing macrophages *in vitro* whose behavior and characteristics closely resemble primary human macrophages, albeit not perfectly[38]. For example, bone marrow-derived macrophages have increased gene expression of TLR4, TLR2, IL-1β, HIF-1α and IL-6 than THP-1 macrophages, whereas THP-1 macrophages have increased gene expression of TNF-α than bone marrow-derived macrophages[38]. THP-1 cells are also less responsive to LPS than primary monocytes and macrophages, which may be attributed to lower CD14 presence on both the THP-1 monocyte and macrophage membrane, which can be used to heighten sensitivity to LPS through complexing with TLR4[38].

Furthermore, the M2 markers CD206 and CD163 were either present in only a few THP-1 macrophages or not found on the THP-1 macrophages, respectively, resulting in the lower M2-like inflammatory response in THP-1 macrophages in comparison to bone marrow-derived macrophages[38]. However, the expression of the above M2 markers may not be altered in THP-1 macrophages, depending on the exposure to macrophage polarizing agents[40]. These discrepancies not only emphasize the flaws in characterizing macrophages using M1/M2 classifications[40], as macrophage phenotypic plasticity is better described as a range or spectrum of

activations, but they also indicate the range of the THP-1 macrophage phenotypic plasticity and its wide use in understanding human macrophages *in vitro*.

Despite the differences between THP-1 macrophages and bone marrow-derived macrophages, THP-1 cells remain a reliable source to understand human macrophage behavior *in vitro*. Moreover, their easy culturing conditions and ease of access during the COVID-19 pandemic make THP-1 cells an additionally beneficial model organism for a graduate student.

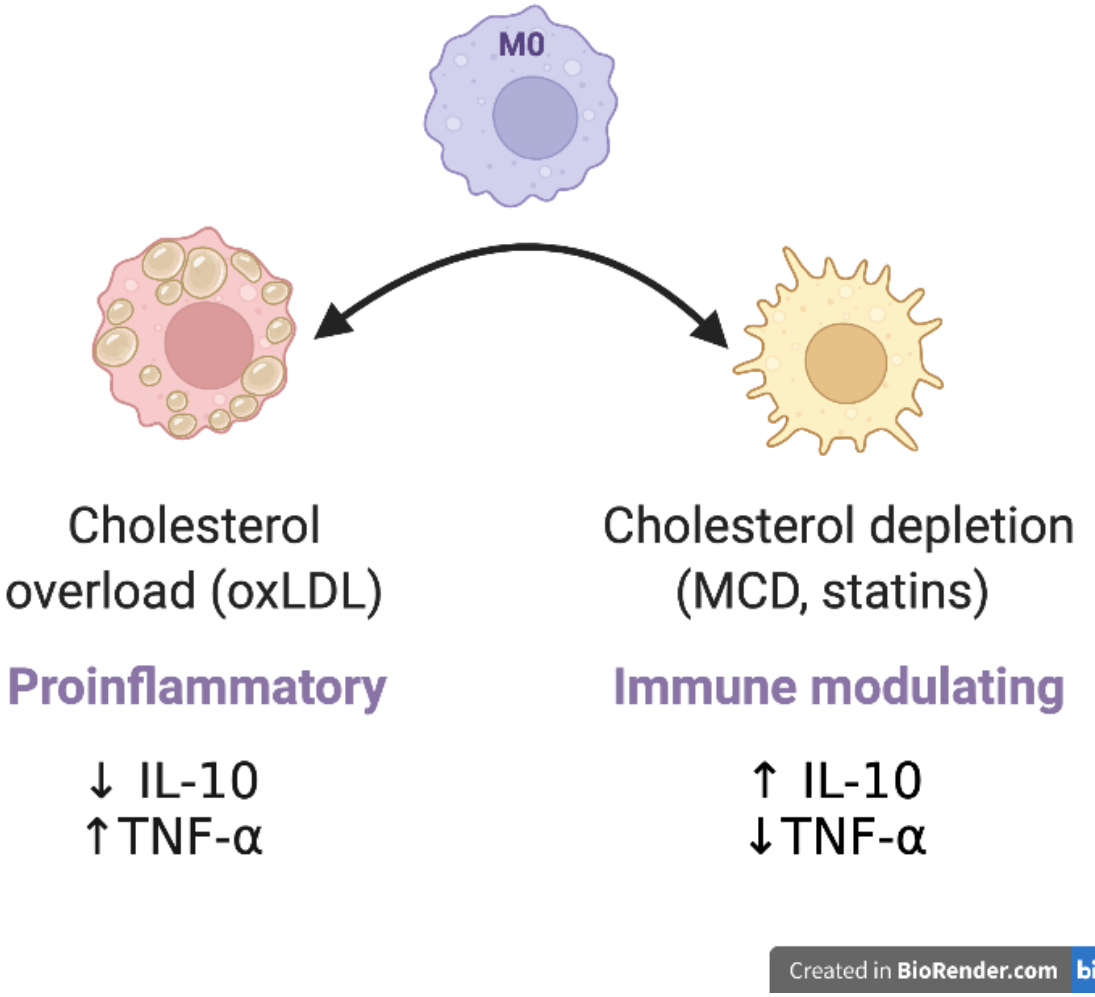

Figure 2. Macrophage polarization is heavily dependent on environmental signals.

Macrophages can display a very diverse plethora of responses to numerous stimulants. In vitro, macrophages are categorized to adopt behaviors ranging from the M1-like (pro-inflammatory) to the M2-like (immune-modulating) subtype. The M1 subtype is induced by molecules such as LPS and oxLDL and is involved in the recruitment of other inflammatory mediators and the release of ROS. The M2 subtype is associated with tissue and wound repair. It is important to note that macrophage phenotypes can diverge from this spectrum of macrophage activation and display either, both or neither phenotypic marker of inflammation. In this project, IL-10 is used as a marker for immune-modulating behavior and TNF-α is used as a marker for pro-inflammatory behavior.

Image created with BioRender.com.

1.3 Cholesterol and LDL: Metabolism and contribution to atherosclerosis

Cholesterol is a four-ring lipid molecule that can either be absorbed from the diet or made *de novo.* This section reviews cholesterol in human macrophages and summarizes the role of cholesterol in atherosclerosis.

1.3.1 Cholesterol metabolism

Cholesterol biosynthesis is largely attributed to the following regulators: SREBP; the sensors for cellular cholesterol, and HMGCR; the rate-limiting enzyme of the mevalonate pathway whose expression is regulated by SREBP2, and the target for all statins[7,55,56]. Many cell types are capable of synthesizing cholesterol, yet the liver supplies half of total *de novo* cholesterol alone to the body[56]. A decrease in cholesterol or extracellular lipids, which can be induced by statins, increases the expression of SREBPs to activate downstream pathways to regulate the expression of genes such as the LDLR[55].

Cholesterol obtained from the diet is first absorbed to the small intestines by the NPC1L1 on enterocytes, where it is packaged into chylomicrons and released into the bloodstream[56]. The chylomicrons are then reorganized in the liver into VLDL, along with cholesterol generated *de novo*, and deposits cholesterol into tissues throughout the body, ultimately decreasing in density, forming LDL. LDL, absorbed by the LDLR, can leak across membranes into spaces such as the arterial intimal subendothelial space to generate fatty streaks at risk of developing into more complex atherosclerotic lesions.

Besides transferring cholesterol to ApoAI or ApoAII to generate nascent HDL during reverse cholesterol transport[57], a process where nascent HDL generated in the liver transports intracellular cholesterol from peripheral tissues to the liver for processing and excretion[58], ABCA1 significantly contributes to the cellular immune responses, where ABCA1 knockout models have shown increased pro-inflammatory responses to stimuli, and accumulate cholesterol at greater levels[59,60]. Maturing HDL can then continue to collect cholesterol from cells through ABCA1 or ABCG1. The expression of ABCA1 and ABCG1 is regulated by miR-33[3], a type of noncoding microRNA that is co-transcribed with SREBP-1a to control cholesterol homeostasis in an SREBP-dependent manner[61]. Two forms of miR-33 exist: miR-33b, which is cotranscribed with SREBP-1, and miR-33a, which is cotranscribed with SREBP-2[62]. miR-33 also influences the expression of AMPK, a protein heavily involved in immune-modulating responses[32]. A decrease in miR-33 was found to increase markers of the M2 state[63]. ABCA1/ABCG1 expression is also regulated by LXR, another nuclear receptor responsible for the regulation of reverse cholesterol transport. In turn, ABCA1 can regulate other compounds, such as PKA, for the activation and transcription of target genes, primarily genes that emphasize the M2 response[50].

1.3.2. Cholesterol in human macrophages

As mentioned above, LDL can be internalized in human macrophages through LDLR. Cholesterol can also be ingested by the SR or LRP families when ingesting modified cholesterol such as oxLDL, as native LDL is not ingested by

SRs[15]. Cholesterol can be used intracellularly to generate cell and organelle membranes, synthesize hormones, regulate gene expression, and can be modified for storage. Excess cholesterol originating from external sources, such as ingestion, promotes lipid droplet formation in macrophages, with *de novo* synthesized lipid sources having little to no incorporation in lipid droplets[23]. These lipid droplets can function to be a storage for phospholipids to be used during phagocytosis, and provide substrates for the synthesis of ATP, nuclear receptors, cell membrane components and eicosanoids[23].

LDLR presence is low on the macrophage plasma membrane when the cell is in environments with, or intracellularly has, excess cholesterol[64]. This is due to the downregulation of the LDLR by directing it to the lysosomes for degradation when coupled with PCSK9, as mentioned above, whose expression is regulated by SREBP-2[56]. Macrophages stimulated with oxLDL in vitro have lower phagocytic capacity, ingesting oxLDL through CD36[18], where oxLDL can also interact with TLR4[65]. Since scavenger receptors are not downregulated by its ligands such as oxLDL or high intracellular cholesterol[64], the macrophage can continue the uncontrolled uptake of modified cholesterol faster than it may be able to metabolize. This gives rise to the progression of atherosclerosis in an uncontrolled manner to stop LDL presence in the arterial intima.

ER stress is also a hallmark characteristic of macrophages overloaded with cholesterol. Extensive ER stress activates the unfolded protein response[66], which can trigger apoptosis in macrophages that are unable to recover from unrestricted cholesterol intake. Moreover, the increase in the production of 25-

hydroxycholesterol, a precursor of cholesterol that has an affinity for LXR[31], is linked to decreased macrophage efferocytosis. Therefore, cholesterol overload not only contributes to the development of atherosclerotic plaques by simply increasing the bulk of the plaque with lipids and recruiting leukocytes, but also worsens atherosclerosis by hindering normal cellular functions such as efferocytosis in macrophages and triggering apoptosis.

Atherosclerosis is a low-grade inflammatory disease[14,44], and using microbial stimulants such as LPS induces a strong, pro-inflammatory polarization in macrophages *in vitro*. LPS stimulation in macrophages also induces an increase in the production of fatty acids because of the increased supply of Acetyl-CoA, produced from citrate, and NADPH, which is produced from the pentose phosphate pathway that is also upregulated by LPS[32]. Furthermore, LPS-dependent NF-κB activation can increase the transcription of NLRP3 inflammasome complex components in an SREBP-dependent manner[32]. The activation of the NLRP3 complex shifts the cell to favor a pro-inflammatory state; LPS-stimulated macrophages display M1-like behavior that includes the secretion of pro-inflammatory cytokines such as IL-1β and IL-18[24], whose production capacity is increased by augmented de novo lipogenesis, and increased phagocytosis[32].

Genes involved in the regulation of cholesterol metabolism were also linked to macrophage inflammatory signaling[67]. CGI-58 is a coactivator of ATGL, and both molecules have significant roles in lipolysis. However, CGI-58 was found to suppress LPS-induced inflammation and mitochondrial dysfunction, measured by oxygen consumption rate, ATP levels and ROS production, through the regulation of PPARγ

in mouse macrophages, a process that was independent of ATGL. The mechanism of CGI-58 modulating PPARγ signaling was determined to be through CGI-58-mediated removal of HDAC2 from the *PPARγ* promoter, and thus maintaining histone acetylation markers for the induction of *PPARγ* expression. This provides evidence that regulators of cholesterol metabolism induce inflammation through epigenetic mechanisms in macrophages.

1.4 Research Problem and Solution Strategies

1.4.1 Research Problem: Rationale for project

The outstanding problem that stimulated this project was that the intracellular mechanisms by which changes in cellular cholesterol concentrations change macrophage outputs are not well characterized in the literature. It is known that the link between cholesterol and macrophage output may be epigenetic due to the significant role of JMJD3 in M2 activation[49], and that oxLDL induces a shift in macrophage cytokine expression and secretion to favor the secretion of pro-inflammatory molecules such as TNF-α.

As stated briefly in previous sections, our laboratories' previous studies[50] show the increased secretion of IL-10 mouse BMDMs, which was shown to be regulated by ABCA1 in a PKA-dependent manner. Consistently, ABCA+/+ BMDM secreted less TNF-α than ABCA1-/- BMDM. Moreover, acute cholesterol depletion through MCD administration was shown to activate PKA in RAW macrophages, which then increased IL-10 and decreased TNF-α secretion upon LPS stimulation. RAW macrophages overloaded with acetylated LDL showed lower PKA activity, and

it also secreted more TNF-α and less IL-10. Therefore, our laboratory previously showed that cholesterol modulates mouse macrophage inflammatory output, favoring the proinflammatory macrophage response upon cholesterol loading, which is consistent with the behavior of macrophages during atherosclerosis development *in vivo*.

The goal of this project was to replicate the above experiments performed by our laboratory that characterize the inflammatory outputs of human macrophages in the presence of MCD + LPS and introduce inhibitors of the proposed signature cholesterol-induced epigenetic priming pathway, such as echinomycin to inhibit HIF-1α. The results of this project would have helped to understand how cholesterol induces inflammation in atherosclerosis.

1.4.2 Research Solution Strategies: Hypothesis and Proposed Model

Acute cholesterol depletion with MCD was hypothesized to increase the expression of HIF-1α, which would lead to the subsequent increase in JMJD3 and JARID1 gene expression, relative to cells not exposed to MCD (Figure 3). The increase in the histone demethylases were hypothesized to remove H3K27me3 for immune modulating genes (represented by IL-10) and H3K4me3 for proinflammatory genes (represented by TNF-α). This is the expected “poised state” of a macrophage treated with MCD prior to the stimulation of LPS. Upon LPS stimulation after MCD pretreatment, the increase in IL-10 relative to TNF-α gene expression and secretion were hypothesized to be reflective of immune-modulating phenotypes; MCD-treated THP-1 macrophages were expected to increase IL-10 gene outputs and decrease

TNF-α gene outputs upon inflammatory stimulus. Thus, the IL-10/TNF-α ratio was hypothesized to increase in macrophages treated with MCD + LPS relative to macrophages treated with LPS alone. The IL-10/TNF-α ratio was used to stabilize the variation of TLR4 presence between cells, samples, and treatments.

1.4.3 Objectives of Study

The first objective was to analyze the changes in IL-10 expression and secretion relative to TNF-α expression and secretion in THP-1 macrophages treated with MCD + LPS, which were quantified using RT-qPCR and ELISA.

Upon the successful completion of the first objective, **the second objective** was to target each molecular marker in the proposed model with inhibitors and stimulate the cholesterol-deprived macrophages with LPS. HIF-1α, JMJD3 and JARID1 were to be inhibited with specific and general inhibitors. However, the first objective, the THP-1 response to LPS and MCD, was not consistently observed across experiments and did not produce consistent results. Therefore, the second objective of this study was not analyzed to its intended extent, with relatively few proof-of-concept experiments performed using echinomycin, a well-characterized and established inhibitor of the HIF-1α protein[68].

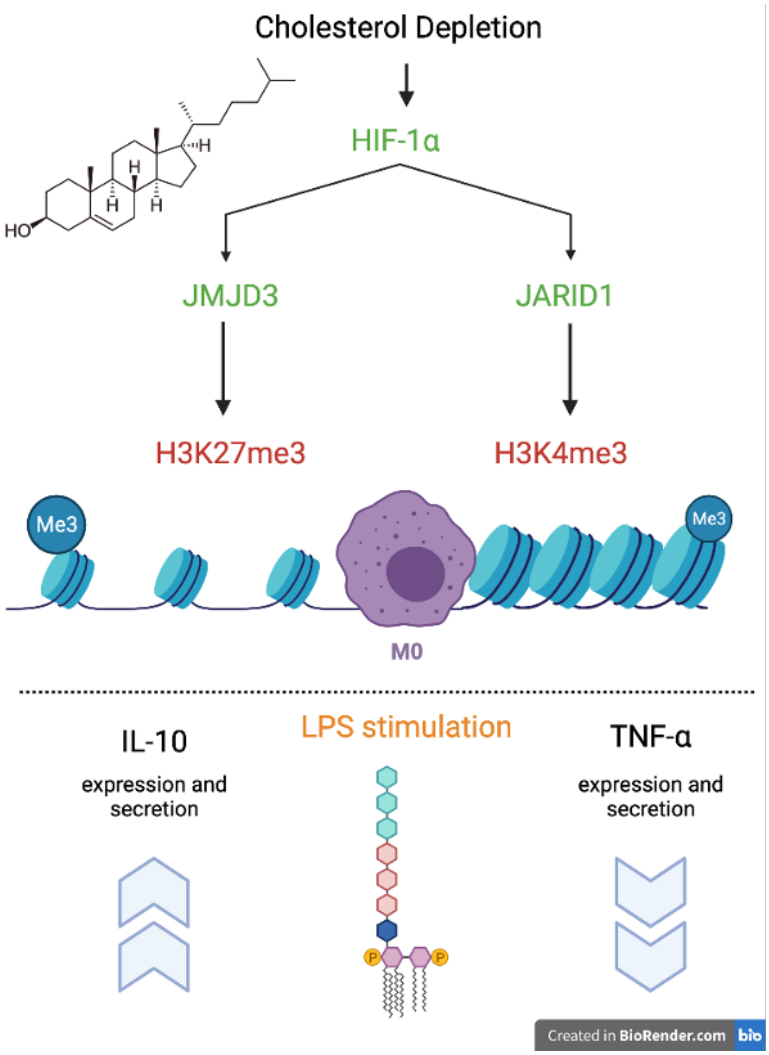

Figure 3. Proposed model: Acute cholesterol depletion is hypothesized to increase IL-10 output relative to TNF-α output in LPS-challenged THP-1 macrophages through epigenetic mechanisms.
Acute cholesterol chelation using MCD is hypothesized to influence the increase in JMJD3 and JARID1 through regulating HIF-1α expression. This is expected to reduce H3K27me3 and H3K4me3, respectively, priming the epigenome before inflammatory challenge. Upon LPS stimulation, an increase in the expression of immune-modulating genes (represented by IL-10) and a decrease in the expression of pro-inflammatory genes (represented by TNF-α) is hypothesized.

Image created with BioRender.com.

1.5 Lay Summary

Atherosclerosis is a chronic disease originating from the buildup of cholesterol in inflammatory and muscle-derived cells within the artery walls and can be the cause of fatal occurrences such as heart attacks or strokes. Macrophages, among other cell types, ingest excess cholesterol to resolve inflammation initiated by leaked LDL beneath the arterial intima. However, unabated lipid consumption results in the formation of a significant portion of the atherosclerotic plaque.

The presence of cholesterol significantly influences macrophage behavior. Therefore, this project sought to describe the effect of cholesterol exerted on human macrophages.

We analyzed the expression and secretion of cytokines in human macrophages acutely depleted of cholesterol and presented with an inflammatory. We also analyzed an enzyme that governs the production of these cytokines, JMJD3. While cholesterol depletion did increase *JMJD3* gene expression, no consistency between the cytokine responses of cells depleted of cholesterol and stimulated with LPS was observed. Future studies should include the characterization of other enzymes that work alongside JMJD3 and other cytokines and characterize these in different human macrophagic cell lines.

CHAPTER TWO: Materials and Methods

2.1 THP-1 Cell Culture

2.1.1 THP-1 cell origin

All THP-1 cells were derived from preexisting cell vials existing in the Drs. Xiaohui Zha and Alexander Sorisky laboratory liquid nitrogen tanks. The cells were not tested for endotoxin or mycoplasma contamination. No new cells were ordered from the ATCC at any point during this study. THP-1 cells were used as a reliable alternative to primary human macrophages. Primary human macrophages were unable to be sourced to the laboratory due to service disruptions during the COVID-19 pandemic.

2.1.2 THP-1 monocyte culture and subculture techniques

THP-1 monocytes were maintained in complete DMEM containing 10% heat-inactivated FBS and 1% PS. The cell concentration was maintained between 3x10^5-1.5x10^6 cells/mL in tissue culture-treated suspension flasks and stored in the tissue culture incubator at 37 C with 5% CO_2. THP-1 monocytes were used to set up experiments between passages 2 and 10 (P2 and P10) and were rarely cultured past P10.

2.1.3 THP-1 differentiation protocol

THP-1 monocytes were adjusted to a concentration of 3x10^5-4x10^5 cells/well for 12-well plates and 1x10^6-1.2x10^6 cells/well for 6-well plates in

complete DMEM. 75 nM PMA was diluted from the stock solution of 1-20 mM PMA in DMSO in fresh complete DMEM, then added to the THP-1 monocytes to be differentiated. The cells were plated immediately after PMA addition and incubated at 37 C with 5% CO_2 for 48 hours. Differentiation from monocyte to macrophage was determined by visual changes under a microscope: THP-1 monocytes are smaller, smoother, rounder and detached; THP-1 macrophages are larger, rougher, flatter and adhered to the plate surface.

THP-1 macrophages were kept in DMEM until fully differentiated. The cells were then washed and covered in 0.25% BSA/RPMI for experimentation. While the ATCC advises THP-1 cells to be cultured in complete RPMI, complete DMEM was used for the culturing of the THP-1 monocytes due to the higher glucose concentration of DMEM for increased cell survival. RPMI was limited for use in experimentation alone.

2.1.4 MCD + echinomycin protocol

THP-1 macrophages were washed with 1X PBS after PMA-induced cell differentiation. 3 or 5 mM MCD and/or 5 nM echinomycin were prepared separately in a tube and added to the cells for 1 hour. MCD was diluted from the 150 mg/mL stock in dH_2O, and echinomycin was diluted from a stock concentration of 1 mM in DMSO. The DMSO negative controls were adjusted to the largest concentration of echinomycin per experiment and the concentration is defined in every figure. DMSO was added as a negative control to all experiments using echinomycin.

2.1.5 LPS + MCD protocol

THP-1 macrophages were washed with 1X PBS once and serum-starved with 0.25% BSA/RPMI for 30 minutes prior to 3 or 5 mM MCD administration for 1 hour in BSA/RPMI. Samples were prepared in a tube separately and administered to the wells unless explicitly indicated otherwise. Preparing the reagents separately prevents the cells from being heavily concentrated with MCD stock (113 mM in dH_2O) in one area and minimizes pipetting errors when administering the MCD volume to the media.

Before LPS stimulation, the cells were washed once with 1X PBS and LPS was administered in 0.25% BSA/RPMI. The cells were incubated with LPS +/- for 3 hours before sample collection. The cells were always washed with PBS after MCD incubation and LPS administration to avoid the complexing of LPS with MCD.

2.1.6 Sample collection protocol

Samples were analyzed under the microscope and cell culture and experiment pictures were taken from a personal mobile phone where applicable.

If using LPS in an experiment, the cell media was collected to determine cytokine secretion. Media was removed from the wells and centrifuged at least 10,000 RCF for 10 minutes. Without disturbing the resulting pellet, the media was then allotted into microfuge tube aliquots and stored in the -80C freezer for future use.

The cells were collected with TRIzol in all samples regardless of treatment. After the removal of cell culture media either with a sterile vacuum tip (for

experiments with no LPS) or careful removal with a pipette into a microfuge tube for downstream ELISA (experiments utilizing LPS), TRIzol was added to the cells and equal coverage was given by hand rotation. Wells were scraped, transferred to a microfuge tube kept on ice and stored in a -80C freezer until future use. The experiment plate was analyzed under a microscope to confirm the lack of cells after TRIzol administration.

2.2 RNA extraction from THP-1 macrophages

The TRIzol lysate was first mixed with a fifth volume of 24:1 chloroform: isoamyl alcohol and incubated on ice for 3 minutes. Once a layer had formed, the samples were centrifuged to separate the layers. The samples were centrifuged at 21,000 rcf for 7 minutes at room temperature by the end of my MSc studies, however, the phase separation and tight packing of the interphase changed from sample to sample.

After centrifugation, the aqueous layer was collected in a separate RNAse-free microfuge tube and mixed with an equal volume of 70% ethanol and mixed thoroughly. This solution was then transferred to the EZ-10 spin column from the BioBasic mammalian RNA extraction kit and centrifuged at 12,000 rcf for 30 seconds. Discarding the flow-through, the columns were washed twice as per manufacturer instructions with wash buffers with added ethanol before their cDNAs empty centrifugation to minimize ethanol contamination.

The RNA was eluted from the columns with 30 uL RNAse free dH_2O after incubating for 2 minutes on ice and taken for nanodrop and downstream processing.

2.3 RNA Nanodrop and Reverse Transcription

2.4.1 Nanodrop machine information

Two nanodrop machines were used throughout this project: the nanodrop in the William Stanford lab, and the ThermoFisher nanodrop in the shared equipment room of the fifth floor Critical Care Wing of the Ottawa Health Research Institute. All results presented in this thesis are derived from samples that were tested with the shared ThermoFisher nanodrop. 1 uL sample was loaded onto the machine after blanking with the diluent (RNAse free dH_2O) and the resulting nucleic acid concentration, A260/280 and A260/230 absorbance ratios, as well as any corrections made automatically by the machine to account for contamination, was retained and these values were used for further processing for reverse transcription for RT-qPCR preparation.

Ensuring the generation of 1 ug cDNA was done with the nanodrop calculations only as cDNA nanodrop is misleading due to the presence of remaining dNTPs in the sample solution.

2.4.2 Reverse transcription of samples

RNA was diluted with RNAse free dH_2O to adjust to 1 ug/sample. 7X gDNA wipeout solution was added and ran in the thermal cycler for 2 minutes at 42 C. Then, 6 uL of the master mix containing the reverse transcription buffer, reverse transcriptase and dNTPs were added per sample. The samples were then reverse transcribed into cDNA for 42 C for 30 minutes and 95 C for 3 minutes. The resulting cDNA was used for RT-qPCR or stored in the -20C freezer for future use.

2.4 RT-qPCR Protocol

cDNA dilutions were determined empirically for IL-10 and TNF-α; cDNA was diluted manually determined by prior observation and experiences. 1 uL diluted cDNA was loaded onto the qPCR plates for a total of 20 uL sample volume, formed by cDNA and the master mix containing SensiFAST lo-ROX SYBR, RNAse free dH_2O and necessary primers. The RT-qPCR was run on the Agilent Aria MX Real-Time PCR Machine (G8830A) and the C_t values were obtained from the same software. Samples of treatments and negative controls were prepared as technical triplicates on one RT-qPCR plate within the same run. Technical triplicates were repeated for both genes of interest and housekeeping controls.

2.5.1 Thermal profile

The thermal profile for RT-qPCR was as follows: 1 cycle of polymerase activation: 2 minutes at 95 C. Followed by 40 cycles of: Denaturation at 5 seconds at 95 C, annealing at 10 or 30 seconds at 55 C, and extension: 20 seconds at 72 C. If a melt curve was performed, the thermal cycle was: 95 C for 30 seconds, 65 C for 30 seconds and 95 C for 30 seconds.

2.5.2 Primer sequences

Primer oligonucleotides were ordered from ThermoFisher (Table 1) and were suspended in RNAse free distilled H_2O to adjust to 100 mmol of primer stock. The aliquots used for RT-qPCR were diluted 1:10 to 10 mmol in RNAse free dH_2O.

Primers were stored at -20C, oligonucleotides were stored at room temperature away from sunlight until suspended in water.

Gene Name	Primer Type	Primer Sequence
Human *HPRT1*	Forward	CAT TAT GCT GAG GAT TTG GAA AGG
	Reverse	CTT GAG CAC ACA GAG GCC TAC A
Human *TNF-α*	Forward	GCC CCC AGA GGG AAG AGT TCC C
	Reverse	CAG CTC CAC GCC ATT GGC CA
Human *IL-10*	Forward	CGA GAT GCC TTC AGC AGA GT
	Reverse	GGC AAC CCA GGT AAC CCT TA
Human *JMJD3*	Forward	ACC CTC GAA ATC CCA TCA C
	Reverse	GTG TTC GCC ACT CGC TTC

Table 1. Primer sequences of genes used throughout the project. All primers were ordered from ThermoFisher/Invitrogen. Oligonucleotides were resuspended in RNAse free distilled water to 100 mmol and diluted in RNAse free distilled water to 10 mmol before use in RT-qPCR. Primers were stored at -20C when suspended in water, otherwise stored at room temperature away from sunlight as oligonucleotides.

2.5 ELISA Protocol

The ELISA protocol was followed as directed by the manufacturer without modification. CoStar 96 9018 plate wells were coated with 100 uL of the detection antibody overnight at 4C. The coated plates were blocked with 1X ELISA buffer and standard solutions, samples and their dilutions were added to the wells. The plates were incubated overnight for maximum absorbance sensitivity. The secondary antibody was then introduced to the wells, followed by the HRP enzyme. TMB solution was added and the stop solution of 2N H_2SO_4 was added once the TMB solution color developed to a mid-tone blue. Wash steps were present between each step, except for the final step between adding TMB solution and stop solution, and the wells were washed with 0.05% PBST (0.05% Tween/1X PBS). The finished ELISA assay components could be assessed by the spectrophotometer for up to two hours after adding the stop solution, however, the assay was always read immediately after adding the stop solution.

The Invitrogen TNF-α kit standard detects 4-500 pg/mL cytokine in media. Media for TNF-α detection was diluted 50 or 100X to retain sample absorbances within the standard curve.

The Invitrogen IL-10 kit standard detects 2-300 pg/mL cytokine in media. Media for IL-10 detection was never diluted to retain sample absorbance values within the standard curve.

2.6 Parameters of Experimental Validity

Only data obtained from valid experiments are presented in Chapter Three: Results. The parameters of experimental validity were standardized by the end of this project and consist of the following rules:

1. RT-qPCR raw C_t values must remain within 20-30 cycles of the amplification curve; all C_t values must be between 20 and 30 (number inclusive).
2. ELISA absorbance values must remain within the ELISA standard sensitivity ranges of TNF-α: 4-500 pg/mL and IL-10: 2-300 pg/mL. Any outstanding value would have been extrapolated, rendering the final concentration unreliable as the amplification of noise would not have been accounted for.
3. RNA A260/230 and A260/280 nanodrop absorbance values must be above 1.8 each. Pure RNA has absorbance readings above 2.0.

Any experiment not adjacent to the above standards was omitted from presentation and interpretation in Chapter 3: Results.

CHAPTER THREE: Results

3.1 MCD induces an increase in *JMJD3* expression in THP-1 macrophages. 10 nM Echinomycin has inconclusive effects regarding the influence of MCD on *JMJD3* expression.

3.1.1 PMA induces the differentiation of THP-1 monocytes to macrophages.

The primary step in every experimental setup throughout this project was the induction of the differentiation from THP-1 monocytes to macrophages using 75 nM PMA.

THP-1 monocytes are a robust cell line originating from a 1-year-old Japanese male infant with acute monocytic leukemia, as described by Tsuchiya *et al.* in 1980[54], and can be differentiated into macrophages and used as an attractive model for this study due to their close resemblance to primary human monocyte-derived macrophages.

Figure 4A shows freshly subcultured P3 THP-1 monocytes in suspension at 40X magnification on a light microscope and Figure 4B shows PMA-induced, fully differentiated P2 THP-1 macrophages in 6-well plates at 20X magnification on a light microscope. The change from monocytes to macrophages was determined by visual examination before removal before experimentation. THP-1 monocytes are smaller, smoother, rounder and are suspended in cell media, whereas fully differentiated THP-1 macrophages, prior to any other treatment, are larger, rougher, flatter and are attached to the plate surface.

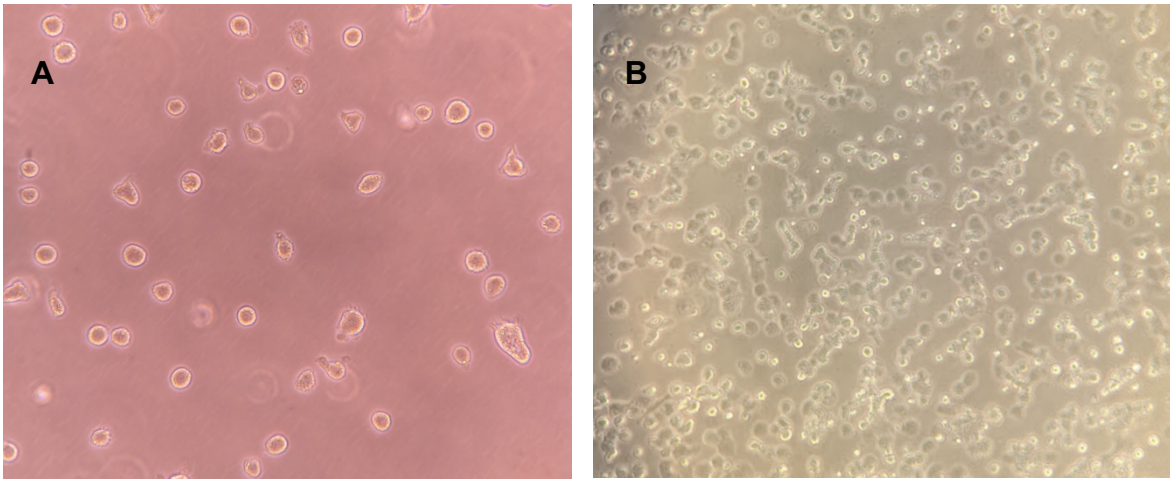

Figure 4. P3 THP-1 monocytes in culture (A) **and differentiated P2 THP-1 macrophages** (B)**.**
THP-1 monocytes (A) were used in cell culture and macrophages (B) were used for experimentation. Monocyte to macrophage differentiation was achieved by administering 75 nM PMA to the desired concentration of cells (300,000-400,000 cells/well for 12-well plates, 1,000,000-1,200,000 cells/well for 6-well plates) for 48 hours in complete DMEM (10% heat-inactivated FBS, 1% PS). Differentiation was determined by visual cues such as cell adhesion, increase in cell size and presence of grooves and protrusions along the macrophage cell membrane. Pictures were taken with a smartphone of THP-1 monocytes and macrophages at 40X and 20X magnification on a light microscope, respectively.

3.1.2 Both 3 mM and 5 mM MCD increase the expression of JMJD3 *in THP-1 macrophages. 10 nM echinomycin has inconclusive effects on JMJD3 gene expression.*

Testing the effect of MCD on macrophage epigenetic mediators is the foundation of this project and was first tested by analyzing the changes in *JMJD3* expression under the influence of MCD. Then, inhibiting the MCD-induced changes with the HIF-1α inhibitor, echinomycin, was attempted. The treatment was not confirmed using total cellular quantification as only RT-qPCR results were used in determining the effect of MCD on THP-1 macrophages.

THP-1 macrophages were treated with 3 mM MCD for one hour. Figure 5A shows that THP-1 macrophages treated with 3 mM MCD displayed an increased JMJD3 gene expression of a 5.7-fold increase relative to BSA/RPMI negative controls.

Having demonstrated that MCD increases *JMJD3* expression in THP-1 macrophages, the proposed model pathway (Figure 3) was tested using inhibitors of the upstream regulators of JMJD3, such as HIF-1α. The inhibition of the HIF-1α protein using 10 nM echinomycin was expected to decrease *JMJD3* expression in THP-1 macrophages, and ideally restoring basal-level gene expression. Because no other HIF-1α target was quantified alongside JMJD3, the effectiveness and validity of echinomycin could not be determined.

THP-1 monocytes were treated with 5 mM MCD for 1 hour, which increased JMJD3 gene expression of 3.6-fold (Figure 5B). Cells that were treated with 5 mM

MCD and 10 nM echinomycin for 1 hour displayed a 3.3-fold increase in JMJD3 gene expression.

The concentrations of echinomycin used throughout this chapter were determined through a preliminary titration of 1 nM-100nM echinomycin, where 10 nM echinomycin reduced the fold change in JMJD3 gene expression to basal levels. However, the titration was retroactively omitted from inclusion in this chapter later in this project due to its classification as invalid determined by the parameters outlined in Chapter 2.6.

This section demonstrates that acute cholesterol depletion by the addition of MCD to the cell media is associated with the increase in the gene expression of histone demethylase JMJD3. However, the effects of echinomycin on JMJD3 gene expression remain inconclusive.

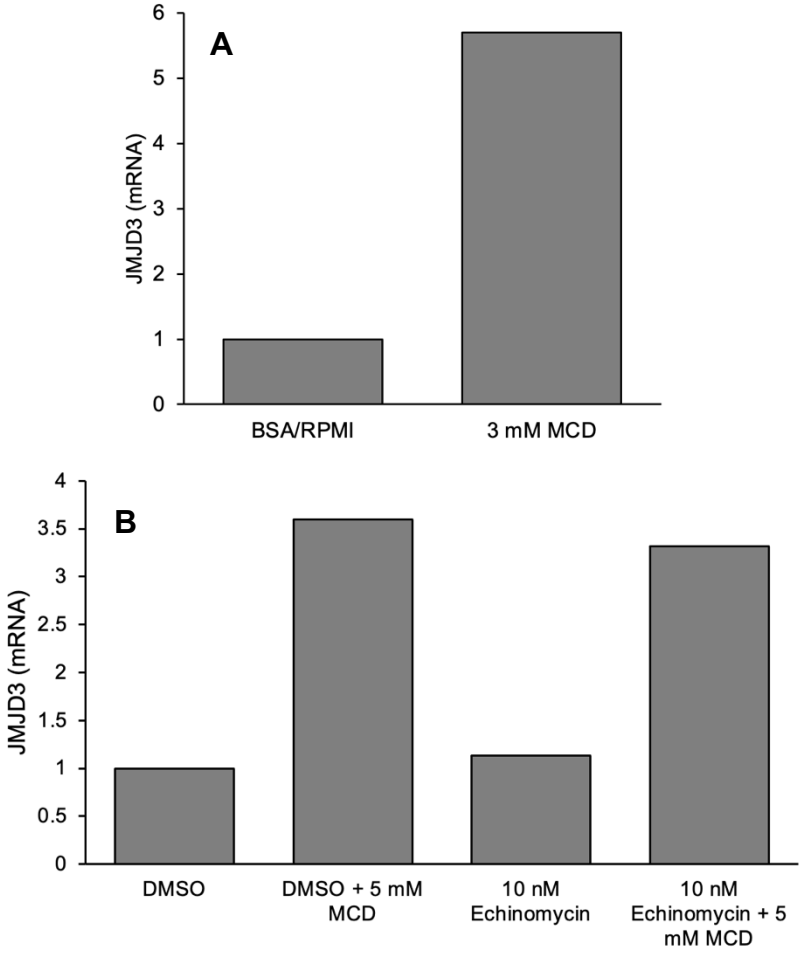

Figure 5. Both 3 and 5 mM MCD increase JMJD3 gene expression in THP-1 macrophages. The effect of echinomycin on JMJD3 gene expression is inconclusive.

THP-1 macrophages were treated with 3 mM (A) or 5 mM (B) MCD in 0.25% BSA/RPMI for one hour. Panel B also shows macrophages co-treated with 10 nM echinomycin (DMSO v/v 10 nM echinomycin).

JMJD3 gene expression increased by 5.7-fold in THP-1 macrophages incubated with 3 mM MCD for one hour (A), however, it only increased to 3.6-fold in another experiment using 5 mM MCD (B).

Moreover, 10 nM echinomycin was not sufficient to decrease this amount despite using the higher concentration of MCD (B).

RT-qPCR results were normalized to the housekeeping gene, *HPRT1*, and to the BSA/RPMI or DMSO negative controls to calculate the fold change in gene expression.

n=1 for each panel; Panel A and B are separate experiments.

3.2 MCD pretreatment in THP-1 macrophages results in an inconsistent inflammatory response upon LPS stimulation.

The next step in this project was to stimulate the primed THP-1 macrophages with LPS to produce an inflammatory response and subsequently characterize the changes in IL-10 and TNF-α outputs.

Only a select few experiments performed throughout the entirety of this project fit all the criteria of a valid experiment and yet produced different results. For example, given pure RNA, in-range C_t and ELISA absorbance values as described in Chapter 2.6, Figure 7 shows the increase in IL-10 and decrease in TNF-α gene expression in cells treated with LPS and MCD. Contrarily, Figure 9 shows that both IL-10 and TNF-α secretions decrease in cells stimulated with LPS following incubation with MCD.

This consistent discrepancy between the experiments described in this subsection provides evidence that the inflammatory response to MCD + LPS treatment in the THP-1 macrophages used throughout this study is inconsistent. Therefore, the hypothesis that inflammatory stimulation following acute cholesterol depletion in THP-1 macrophages increasing IL-10 and decreasing TNF-α gene expression and secretion relative to macrophages that were stimulated with LPS but not depleted of cholesterol cannot be confirmed nor denied, despite the IL-10/TNF-α ratio increasing in all but one of the experiments comparing LPS and MCD+LPS responses.

Drugs administered to the cells, such as MCD or echinomycin, are prepared in a microfuge tube and mixed with 0.25% BSA/RPMI before its administration to the

samples, as described in Chapter 2. However, the results for Figure 6 were generated using cells that had been administered MCD directly to the wells. While this method is not recommended for any drug addition to experimental wells, it was done in this case to avoid any potential interaction of MCD with the microfuge tube, if any, that might have been causing the inconsistencies in IL-10 and TNF-α outputs in the presence of LPS and MCD as described above. The risks of this method outweigh its benefits and are not recommended for laboratory use. MCD is a water-soluble, acute chelator of cholesterol, and therefore the site of drug administration in the well can become overwhelmed with the drug at concentrations greater than its intended delivery (113 mM stock concentration in dH_2O). This can have cytotoxic effects, and the risk of manual error is amplified as thorough pipetting is required to evenly distribute MCD throughout the media in the plate wells. All other figures present experiments whose results were obtained by pretreating THP-1 macrophages with MCD diluted in a microfuge tube before administration.

RT-qPCR results of Figure 6 show a 157.6-fold increase in TNF-α gene expression (Figure 6A), and a 13.9 fold increase in IL-10 gene expression (Figure 6B) in THP-1 macrophages treated with LPS alone. Cells that were treated with 5 mM MCD before LPS stimulation showed a 66.4-fold increase in TNF-α and a 35.7-fold increase in IL-10 gene expression. The resulting IL-10/TNF-α ratios for the RT-qPCR values (Figure 6C) show a value of 0.09 to in LPS-treated macrophages, and a value of 0.54 in macrophages treated with MCD + LPS.

ELISA data produced from the same experiment show the increase in both TNF-α (Figure 6D) and IL-10 (Figure 6E) cytokine secretion in the MCD + LPS group

relative to the LPS group. Cells treated with LPS alone secreted 7687 pg/mL TNF-α and 11.4 pg/mL IL-10, whereas cells pretreated with MCD secreted 10132 pg/mL TNF-α and 31.6 pg/mL IL-10 upon 3 hours of LPS stimulation. The IL-10/TNF-α ratios for this assay (Figure 6F) also increase, with LPS-treated macrophages displaying a ratio value of 0.0015. The ratio increases in macrophages with MCD + LPS to a value of 0.0031.

A second experiment utilizing both 3 mM and 5 mM MCD prior to stimulation with LPS +/- shows the increase in IL-10 cytokine secretion (Figure 7B) in THP-1 macrophages from 17.5 pg/mL in the LPS control (without MCD) to 28.6 pg/mL when pretreated with 3 mM MCD and 30.9 pg/mL when pretreated with 5 mM MCD prior to LPS stimulation. Furthermore, TNF-α secretion (Figure 7A) was observed to decrease in the same samples, with 12571 pg TNF-α/mL secreted in LPS controls (without MCD), and 5262 pg/mL with 3 mM MCD + LPS and 5630 pg/mL with 5 mM MCD + LPS. The minimal difference between using 3 mM and 5 mM MCD is also reflected in the IL-10/TNF-α ratios (Figure 7C): the ratio for the “3 mM MCD + LPS” group is 0.00544, and for the “5 mM MCD + LPS” group, the ratio is 0.00549. The ratio for the LPS+ control group is 0.00139.

In a third independent experiment, LPS stimulation of THP-1 macrophages induced a 79.3 fold and 17.7 fold increase in TNF-α (Figure 8A) and IL-10 (Figure 8B) gene expression, respectively. Administration of 5 mM MCD decreased TNF-α gene expression to increase by only 20.9 fold and IL-10 gene expression to increase 6.6 fold relative to BSA/RPMI controls. Nevertheless, the IL-10/TNF α ratio increased, as evident in Figure 8C. The ratio was 0.22 in cells treated with LPS alone

and increased to 0.32 in cells treated with MCD + LPS. In this experiment, MCD was prepared in a tube and added to the cells for 1 hour in 0.25% BSA/RPMI.

The above results provide evidence for the lack of a difference between administering 3 mM or 5 mM MCD, as evident by the extremely similar IL-10/TNF-α ratios in Figure 7C. Initially, 3 mM MCD was used to provide the cells with the lowest concentration to provide a specific response but was later changed to 5 mM MCD for increased presence of MCD inside the wells, as described in Chapter 3.4.

All the experiments described above show an increase in the IL-10/TNF-α ratio in MCD + LPS groups relative to wells treated with LPS alone. Mathematically, a ratio can increase if the value of the numerator is greater than the value of the denominator. However, the ratio can also increase if there is an increase in the numerator while there is no change in the value of the denominator between comparison groups. Ratios can also increase if the decrease in the denominator is lesser than the value of the increase in the numerator.

Likewise, a ratio can decrease if the decrease in the numerator is greater than the denominator, or if the denominator increases relative to the numerator, or if the denominator increases while the numerator remains constant. While the IL-10/TNF-α ratio accounts for TLR4 variations between samples, thus controlling for the discrepancies between each treatment group cytokine output, this ratio must be considered alongside the individual cytokine values because of the various causes that result in similar ratio outcomes, as described above.

In Figure 9, THP-1 macrophages were treated with 3 mM MCD and/or 5 nM echinomycin before LPS stimulation. DMSO + LPS stimulation increased TNF-α

secretion (Figure 9A) in THP-1 macrophages to 2551 pg/mL, whereas macrophages pretreated with DMSO + 3 mM MCD + LPS secreted 730 pg/mL TNF-α. DMSO + LPS stimulated macrophages also secreted 18.7 pg/mL IL-10 (Figure 9B), whereas macrophages treated with DMSO + LPS + MCD secreted 4.5 pg/mL IL-10. Both IL-10 and TNF-α decreased with DMSO + LPS + MCD treatment, and the resulting IL-10/TNF-α ratio (Figure 9C) for macrophages treated with DMSO + LPS only was 0.007, and macrophages treated with DMSO + MCD + LPS had a IL-10/TNF-α ratio of 0.006.

Because IL-10 did not increase while TNF- α decreased between LPS+ control and MCD+ LPS treatment groups, samples containing echinomycin are not reported for this experiment.

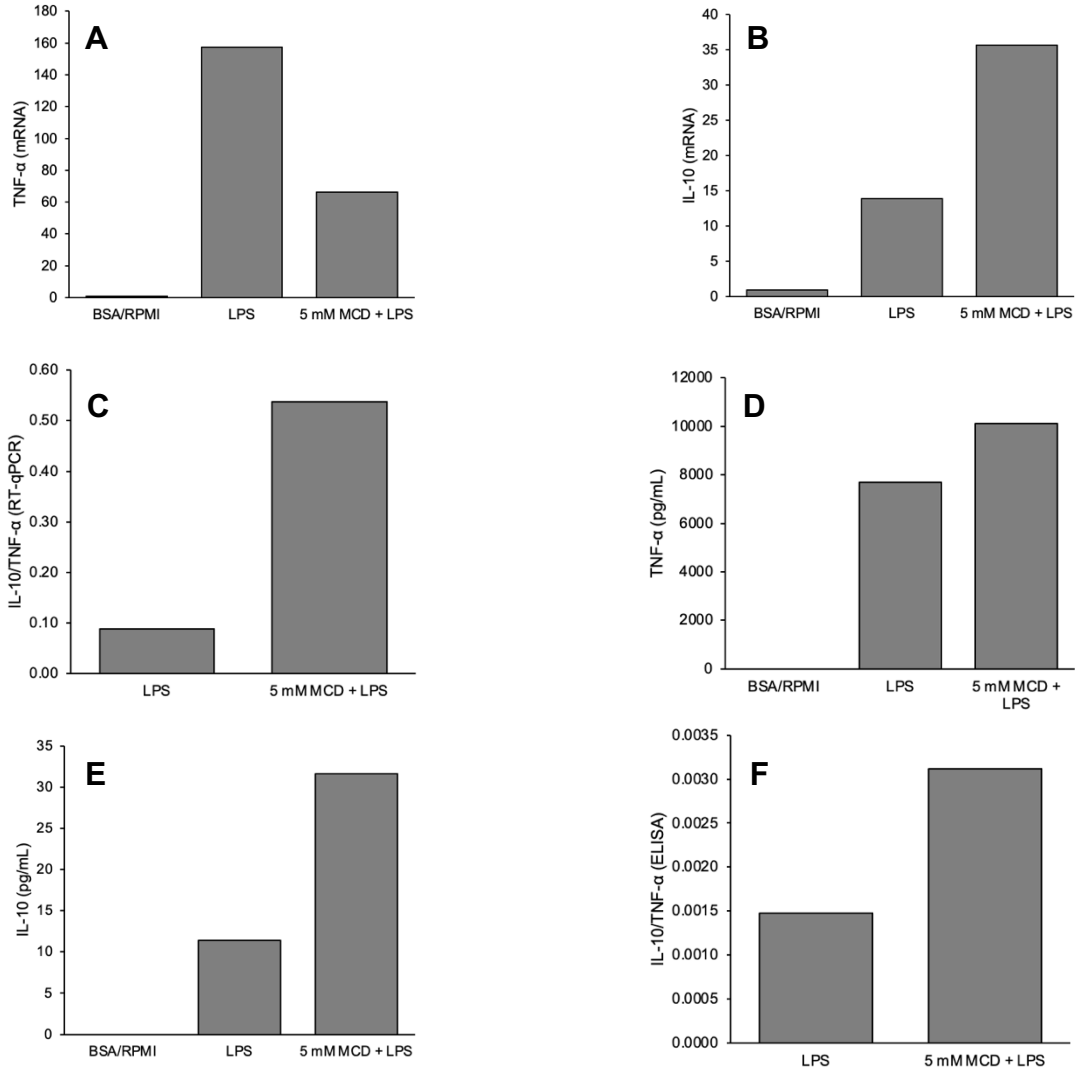

Figure 6. THP-1 macrophages pretreated with 5 mM MCD prior to LPS treatment show an increase in the IL-10/TNF-α ratio.

THP-1 macrophages were treated with 5 mM MCD for one hour prior to inflammatory stimulation with 100 ng/mL LPS for three hours.

MCD + LPS treatment in THP-1 macrophages induces an increased expression in *IL-10* (B) and decreased expression in *TNF-α* relative to the LPS group (A), whereas both cytokines are shown to have increased secretion after MCD + LPS stimulation (D, E). Both RT-qPCR (C) and ELISA assays (F) show the increase in IL-10/TNF-α ratios.

Media was diluted 1:50 for the TNF-α ELISA assay, and not diluted for the IL-10 ELISA assay.

RT-qPCR values were assessed relative to the BSA/RPMI negative control to determine fold change and normalized to the housekeeping gene *HPRT1*. n=1.

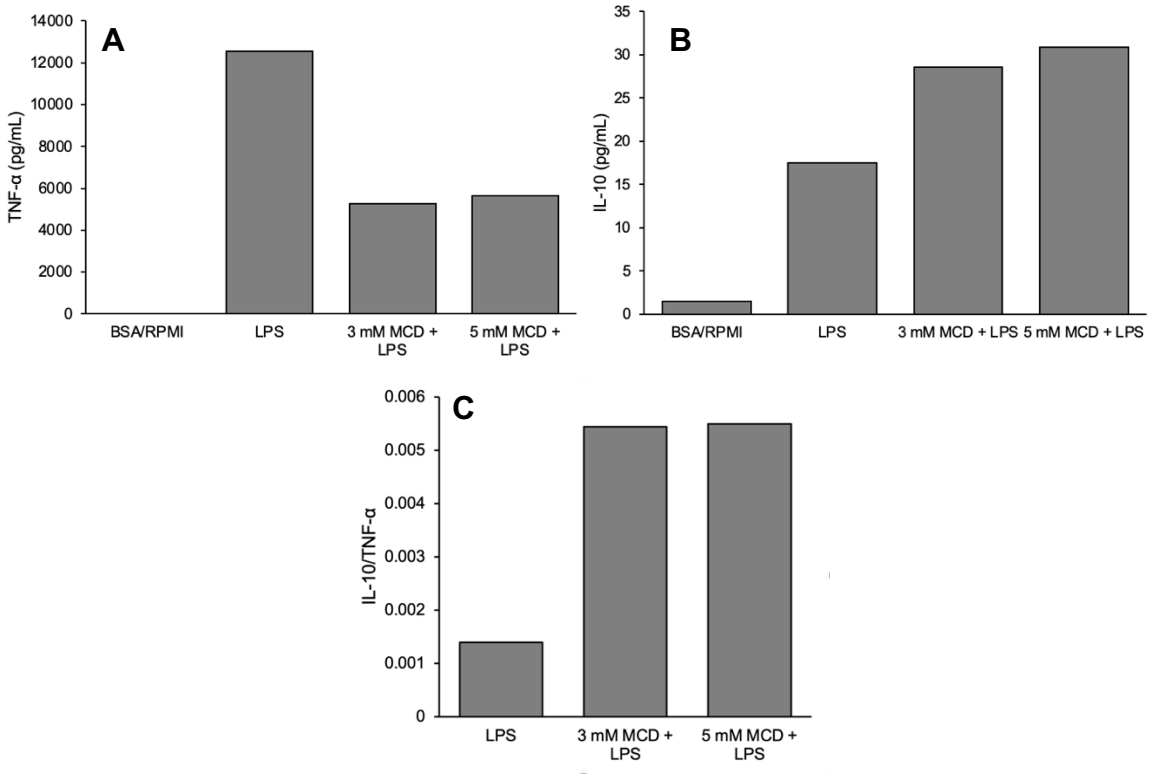

Figure 7. Cholesterol-depleted THP-1 macrophages secrete more IL-10 and less TNF-α upon LPS stimulation relative to the LPS control group.
THP-1 macrophages were treated with 3 or 5 mM MCD for one hour prior to inflammatory stimulation with 100 ng/mL LPS for three hours.
Priming the THP-1 epigenome by pretreating the cells with 3 mM or 5 mM MCD for 1 hour prior to LPS stimulation induces ~1.5-fold increase in IL-10 secretion (B) and a near twofold decrease in TNF-α secretion relative to LPS+ controls (A). Using 3 or 5 mM MCD did not vary the outcome of neither IL-10 nor TNF-α secretion by large quantities. This is also reflected in the very similar cytokine secretion ratios (C).
Media was diluted at 1:100 for the TNF-α ELISA assay and was not diluted for the IL-10 ELISA assay. n=1.

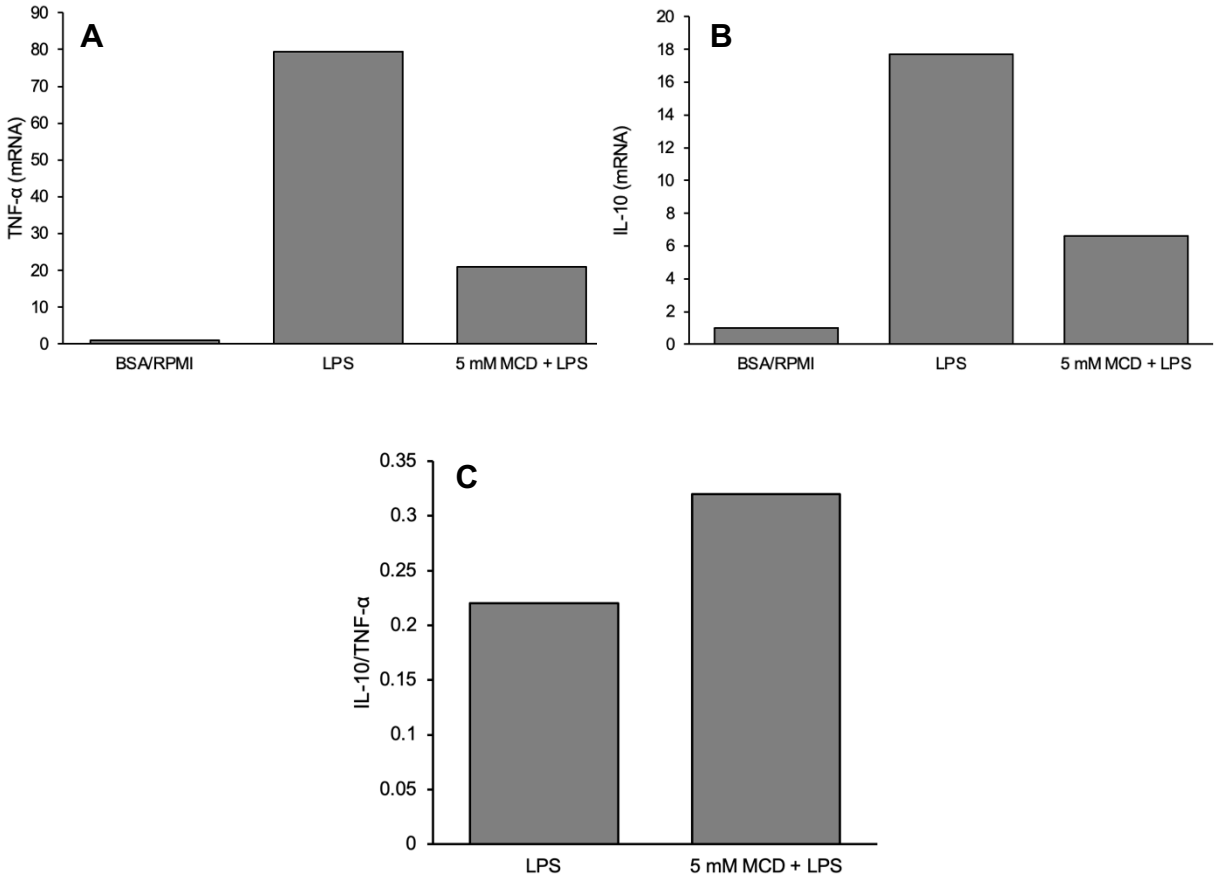

Figure 8. THP-1 macrophages stimulated with LPS decrease IL-10 and TNF-α expression. The increase in the IL-10/TNF-α cytokine ratio is maintained between LPS+ and MCD + LPS treated groups.

Macrophages treated with MCD + LPS express lower cytokine concentrations for both *IL-10* and *TNF-α*. LPS treatment caused 79.3-fold increase, and MCD + LPS treatment resulted in 20.9-fold increase in TNF-α gene expression (A).

Despite the same protocol as previous figures, *IL-10* expression does not increase in MCD + LPS groups (B). MCD + LPS treatment caused a 6.6-fold increase in IL-10 gene expression and a 17.7-fold increase in cells stimulated with LPS alone.

The IL-10/TNF-α ratio increased to 0.32 in cells treated with MCD + LPS from 0.22 in cells treated with LPS alone (C).

RT-qPCR was performed to measure the fold change differences between treatments relative to BSA/RPMI negative controls. All samples were normalized to the *HPRT1* housekeeping gene. n=1.

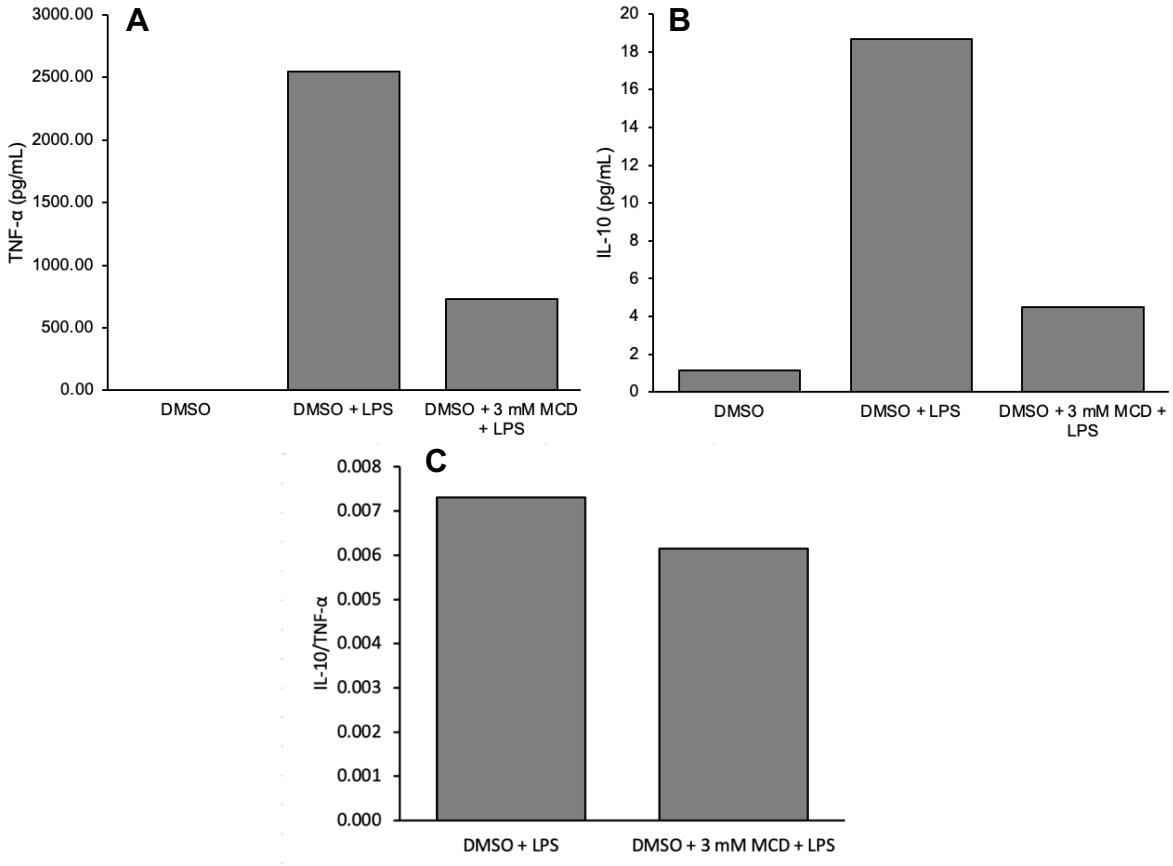

Figure 9. MCD pretreatment in THP-1 macrophages decreases both IL-10 and TNF-α secretion.

Fully differentiated THP-1 macrophages were treated with 3 mM MCD and/or 5 nM echinomycin for 1 hour. The macrophages were then stimulated with 100 ng/mL LPS for 3 hours.

3 mM MCD + LPS decreased both IL-10 and TNF-α secretion relative to LPS treatment alone: IL-10 secretion decreased from 18.7 pg/mL in LPS+ controls to 4.5 pg/mL in cells treated with MCD + LPS (B), whereas TNF-α secretion (A) decreased from 2551 pg/mL to 730 pg/mL in the same groups, respectively. This resulted in a decrease in the IL-10/TNF-α ratios between the LPS+ and the MCD + LPS groups (C).

Because objective 1 of the proposed model was not met, there was no scientific basis for evaluating objective 2, the response of cells to LPS in the presence of MCD + Echinomycin.

The IL-10 and TNF-α secretion analysis was performed using ELISA. Cell experimental media was diluted at 1:50 for the TNF-α assay, whereas the media was not diluted for the IL-10 assay. DMSO negative control v/v equal to 5 nM echinomycin. n=1.

3.3 Echinomycin induces inconclusive effects on THP-1 macrophages treated with MCD and LPS.

Echinomycin was administered numerous times at various concentrations to the THP-1 macrophages throughout this project, however, this thesis presents only figure, utilizing 5 nM echinomycin to counteract the effects of MCD, for this section. Echinomycin treatments were analyzed only on the conditions that IL-10 gene expression/secretion increases and TNF-α gene expression/secretion decreases in macrophages treated with MCD and LPS relative to the LPS negative control group, in addition to meeting the experimental validity criteria as defined in Chapter 2.6.

THP-1 macrophages were treated with 3 mM MCD and/or 5 nM echinomycin and stimulated with LPS. Figure 10B shows the increase in IL-10 secretion to 16.7 pg/mL in THP-1 macrophages challenged with LPS + DMSO. This secretion of IL-10 was further enhanced to 25.3 pg/mL in cells that were pretreated with DMSO and 3 mM MCD before LPS stimulation. Conversely, 1911.4 pg/mL TNF-α was secreted in THP-1 macrophages stimulated with LPS + DMSO (Figure 10A). TNF-α secretion was then reduced to 805.1 pg/mL in macrophages pretreated with DMSO and MCD before LPS administration. All control groups lacking echinomycin were treated with DMSO (v/v equal to 5 nM echinomycin diluted from a stock solution of 1 mM in DMSO).

Coincubation of 5 nM echinomycin with 3 mM MCD minimally affected TNF-α secretion upon LPS treatment. Figure 10A shows the secretion of TNF-α in this condition, 580.7 pg/mL. This provides evidence for 5 nM echinomycin being a

concentration too low to induce a change in TNF-α expression when preincubated with 3 mM MCD.

Conversely, IL-10 secretion was significantly decreased to 10.5 pg/mL in the MCD + echinomycin + LPS group compared to a concentration of 25.3 pg/mL in the MCD + LPS + DMSO control group. This result shows support for 5 nM echinomycin reducing the effect of MCD on IL-10 expression, though the concentration of echinomycin may be too high due to IL-10 secretion values being lower than the basal level of 16.7 pg/mL in the DMSO + LPS group.

Figure 10C shows the increase in the IL-10/TNF-α ratio upon MCD pretreatment: The IL-10/TNF-α ratio was calculated as 0.009 in cells treated with LPS and DMSO, and 0.0314 in cells treated with DMSO, MCD and LPS. As illustrated in Figure 10C, 5 nM echinomycin co-incubated with MCD decreased the IL-10/TNF-α ratio by 1.7-fold relative to cells pretreated with only MCD and DMSO prior to LPS stimulation. However, this ratio conceals the increase of the numerical value of the ratio being attributed to the larger change in IL-10 secretion and the smaller change in TNF-α secretion.

While each cytokine is analyzed individually among treatment conditions, it is crucial to note that IL-10 and TNF-α cannot be interpreted separately as that would introduce bias in data analysis; the response of TLR4-mediated inflammation upon acute cholesterol depletion is only correctly represented through the simultaneous interpretation of both IL-10 and TNF-α.

This section concludes that further testing with echinomycin is required, including assays validating the echinomycin drug itself.

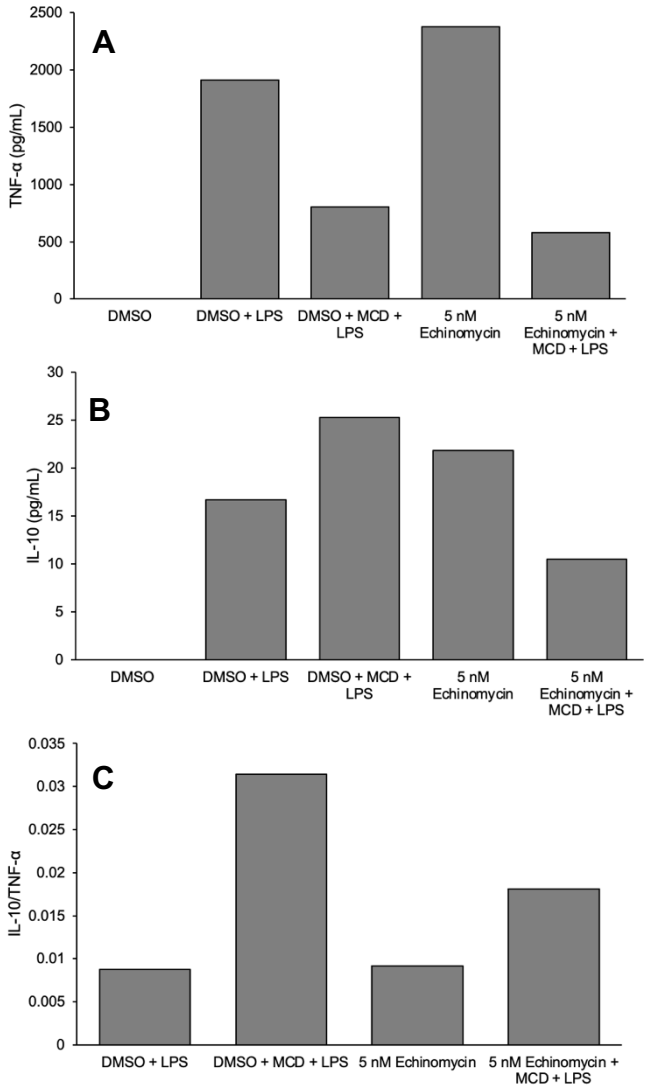

Figure 10. 5 nM Echinomycin reduces the effect of MCD on IL-10 but not TNF-α secretion in LPS-stimulated THP-1 macrophages.
THP-1 macrophages were pretreated with 3 mM MCD and/or 5 nM echinomycin for 1 hour before a 3-hour inflammatory stimulation with 100 ng/mL LPS.
MCD + LPS treatment increased IL-10 secretion relative to LPS treatment alone (B), whereas TNF-α decreased in the same group relative to its negative control (A). Echinomycin + MCD + LPS treatment decreased IL-10 but did not affect TNF-α secretions relative to the MCD + LPS group. As a result, the IL-10/TNF-α ratio (C) shows the decline in the echinomycin + MCD + LPS group relative to the MCD + LPS group. The effect of 5 nM echinomycin on MCD + LPS-induced cytokine secretion is determined to be inconclusive given the inconsistent effects of echinomycin on IL-10 and TNF-α outputs.
DMSO addition v/v equal to 5 nM echinomycin. Cell culture was diluted at 1:50 for the TNF-α assay but was not diluted for the IL-10 assay. n=1.

3.4 Improving experimental quality

The above series of experiments resulted in widely differing results despite the same inputs. Cells are simple yet complex machinery and any observations in their varying outputs must be due to differences unaccounted for prior/during experimentation or during the ELISA or RT-qPCR sample preparation process.

Throughout experimentation, especially in the last few months of this project, significant adjustments were made to the experimental layouts and executions:

First, THP-1 monocytes were shifted from being differentiated in 12-well plates to 6-well plates to allow for more RNA yield, because the differences in downstream results may have been due to low RNA yield harvested before sample processing. The RNA harvested from 12-well plates was low yield after experimentation (Table 2), therefore experimental setup was changed to utilizing 6-well plates for experiments in THP-1 macrophages in the later months of this project. This increase in plate size increased the cell number per well capacity and resulted in more RNA harvested from more cells during TRIzol RNA extraction. Table 2 shows the increase in the RNA in the 6-well plate samples than the 12-well plate samples considering the same treatments of 3 mM MCD for 1 hour and 100 ng/mL LPS for 3 hours, despite different amounts of TRIzol used per well per sample.

Second, the macrophage MCD treatment changed from 3 mM to 5 mM MCD. As noted in Figure 7, there was no significant difference between using 3 mM MCD and 5 mM MCD. Therefore, earlier experiments were performed using 3 mM MCD to obtain a cellular response using the lowest amount of drug. However, the MCD

concentration used in later experiments was changed to 5 mM MCD for increased presence of MCD within the media.

Third, the source of LPS added to wells was changed. Because JMJD3 gene expression increased upon MCD pretreatment, the discrepancy of cytokine responses was narrowed to the production of the individual cytokine and not the upstream regulatory processes. LPS is stored in 0.1 mg/mL aliquots, with a stock concentration of 1 mg/mL. We hypothesized that diluting LPS from a higher stock might induce a different response because drugs stored at higher concentrations do not degrade as easily as their lower concentration aliquots. However, results obtained from macrophages that were stimulated with 100 ng/mL LPS from 1 mg/mL are not reported in this results section because the resulting C_t values were not in range, therefore were deemed experimentally invalid.

Primary human macrophages were used once in this project, which were obtained during the summer of 2020 by my blood donation. However, the resulting RNA harvested from these primary cells was impure and not suitable for downstream RNA-based applications. Therefore, only results obtained from THP-1 macrophage experimentation are presented in this thesis.

	6-well plate (1,000,000 cells/well)			12-well plate (400,000 cells/well)		
Sample Name	**Nucleic Acid(ng/uL)**	**A260/A280**	**A260/A230**	**Nucleic Acid(ng/uL)**	**A260/A280**	**A260/A230**
DMSO	303.97	2.07	2.12	73.93	1.99	2.04
DMSO + LPS	215.80	2.06	2.08	75.02	1.98	1.98
DMSO + MCD + LPS	159.85	2.05	2.02	52.24	1.88	1.54
5 nM Echinomycin + LPS	292.81	2.08	2.10	49.28	1.59	0.41
5 nM Echinomycin + MCD + LPS	142.83	2.07	2.01	45.96	1.80	0.67

Table 2. Increasing well size from 12- to 6-well plates allows for more RNA yield.
THP-1 macrophages were treated with 5 nM echinomycin and/or 3 mM MCD for 1 hour and stimulated with 100 ng/mL LPS for 3 hours. The cell lysate was collected with TRIzol.
Compiled from two independent experiments as representative results for samples originating 6- and 12-well plates, low RNA yield was detected by the ThermoFisher nanodrop machine from samples originating from 12-well plates. Such representative results incentivized the transition from 12-well plates to 6-well plates. The 6- and 12-well plates originate from different THP-1 macrophages at different timepoints. n=1 for each experiment.

3.5 Summary of Results

In this chapter, evidence for cholesterol depletion in THP-1 macrophages using 3 or 5 mM MCD increasing JMJD3 gene expression is shown. However, 10 nM echinomycin inhibiting the effect of MCD on JMJD3 gene expression was not observed, as per Figure 5.

While LPS was able to increase the gene expression of both IL-10 and TNF-α in THP-1 macrophages, the administration of LPS after MCD pretreatment did not produce a consistent outcome. In the experiment with increasing IL-10 and decreasing TNF-α outputs in response to LPS + MCD, 5 nM echinomycin also displayed inconclusive results on the resulting IL-10 and TNF-α secretion. This study concludes that the effect of MCD on human macrophage inflammatory output is inconclusive, and more testing with new THP-1 cells is required.

As discussed in Chapter 4, the reason for these discrepancies may be attributed to the following factors:

- Differences in RT-qPCR and ELISA setup.
- Gene expression and secretion may not be linearly correlated, and upstream regulators (such as JMJD3) may not be altered by the same factors in the same levels of intensity.
- The THP-1 monocytes cells are too old, with some cultures originating from vials stored in the liquid nitrogen tank as early as 2005.

CHAPTER FOUR: Discussion

This study contributed to the understanding of the characterization of the molecular elements that gave rise to the changes in the cytokine expression in LPS MCD macrophages. The goal of this study was to use a small amount of MCD to increase JMJD3 gene expression and to demonstrate the change in IL-10 and TNF-α gene expression/secretion, without affecting the regular functions of the cells. Echinomycin was required to remove only the effect of MCD on JMJD3, IL-10 and TNF-α outputs and restore basal level of gene expression.

The results of this thesis show that while MCD increases JMJD3 gene expression in THP-1 macrophages, the response of LPS-stimulated macrophages pretreated with MCD and/or echinomycin is inconsistent, and that further investigation is required.

4.1 Rationalizing the experimental validity parameters

As described in Chapter 2.6, all results presented in Chapter 3 of this thesis were assessed with RT-qPCR and ELISA under the following circumstances for experimental validity:

RNA nanodrop values for A260/280 and A260/230 must not be lower than 1.8. This parameter is important because common contaminants like phenol (present in TRIzol) or proteins can skew the absorbance values as they also absorb at similar wavelengths, thus resulting in an incorrect RNA concentration reading[69]. As such, inaccurate RNA readings can lead to incorrect cDNA conversion calculations due to

over- or underestimating the actual amount of RNA present. Because each RNA nanodrop reading is unique to its own sample, this results in not only the incorrect amount of cDNA loading onto the qPCR plate, but also can cause differences in the concentration of cDNA loaded for RT-qPCR. Given that all primers and SYBR are added more than what is required of the reaction, the sample cDNA remains the limiting reagent in an RT-qPCR plate. An excess of cDNA causes more copies that are amplified, resulting in lower C_t values, whereas the inverse is true for less cDNA added. Therefore, it is paramount to add the same amount of cDNA across samples, ideally for all assays performed, which cannot be possible if the initial RNA reading does not meet the quality parameters defined earlier.

The reason for progressing with processing samples despite their poor RNA absorbance values that did not meet the criteria was because the shared ThermoFisher nanodrop machine provided corrections of the sample RNA concentration if the purity was low and listed the contaminant causing low purity. In retrospect, the samples should have been discarded immediately despite corrections from the machine and the experiment should have been replicated.

RT-qPCR C_t values must remain within 20-30 amplification cycles (number inclusive). This parameter is important because determining a fold change in the gene expressions between treatment and control samples assumes a linear relationship, which is only achieved if the raw C_t values lie within the exponential portion of the qPCR amplification curve. The lower limit for acceptable C_t values was set to 20 cycles because the RT-qPCR machine determines baseline fluorescence in real time at roughly 15 cycles[70], and the upper limit for acceptable C_t values was

set to 30 cycles because amplification of over 30 cycles indicates the presence of very little cDNA at the start of the assay, where background noise may be misinterpreted as legitimate reads. The C_t value is defined as the number of cycles a sample undergoes to produce copies of the target gene to above the minimum threshold, termed the horizon. The horizon is automatically determined by the RT-qPCR machine for every run.

ELISA values must remain within the cytokine curve of the kit standard solutions. This parameter is important because the ELISA assay kit can only accurately measure absorbance values that lie within the given range of the manufacturer's standard solutions. Any value that is an outlier to these standard values must be extrapolated to fit onto the standard curve. This can result in potentially significant errors in cytokine secretion calculations as noise may be amplified and interpreted as a false-positive cytokine presence in media. The presence of media dilutions can especially exacerbate this phenomenon.

While both RT-qPCR and ELISA are very sensitive tools to determine gene expression and secretion respectively, RT-qPCR is especially sensitive due to the many custom steps introduced throughout this project; Custom primers, cDNA dilution, and thermal profiles were used for RT-qPCR and hence, the use of many modifications may have introduced inconsistencies to the results, despite the customizability of the assay is one of the benefits of using RT-qPCR to determine changes in gene expression. Contrarily, ELISA was performed throughout this project with fewer custom settings; the ELISA assay protocol did not have any modifications to the manufacturer's standard operating procedures.

4.2 Epigenetic changes of acute cholesterol depletion in macrophages

PMA induces THP-1 monocyte to macrophage differentiation through PKC activation, arresting the cells in the G1 cell cycle[71]. Several molecular changes are induced during PMA-mediated THP-1 monocyte differentiation. Functioning as a coreceptor for TLR4[38,72], CD14 is increased on the cell surface in THP-1 macrophages when compared to THP-1 monocytes[73], allowing for a stronger LPS response in differentiated macrophages. Phagocytic capacity also increases relative to THP-1 monocytes due to the increase in CD11b[73,74]. PMA induction in THP-1 macrophages also causes the increase in granularity, namely by increasing the number of mitochondria and lysosomes, and increasing cytoplasmic volume[75]. However, changes between THP-1 monocytes and PMA-induced macrophages do not match the level of changes observed in primary monocyte-derived macrophages. Therefore, THP-1 macrophages are not an exact replacement for monocyte-derived macrophages, which was already discussed in Chapter 1. Despite this, the changes are examples of some of the markers that allow THP-1 macrophages to mimic primary monocyte-derived macrophages and highlight the differences between PMA-induced cell differentiation. A limitation of this project was the lack of the characterization of the change in the molecular markers present in THP-1 macrophages after stimulus with 75 nM PMA for 48 hours in complete DMEM. Experiments described in this thesis utilized only the physical markers of THP-1 monocyte to macrophage differentiation that were clearly observable through light microscopy: flatter and larger shape of the cells with increased granularity compared to THP-1 monocytes, and adherence to the plate surface.

MCD is a seven-ring glucose molecule that solubilizes cholesterol to the media by entrapping cholesterol within its ring structure[76,77]. MCD replaces statins as the method of cholesterol depletion due to its acute effect on cellular cholesterol concentrations; increased incubation times may have uncharacterized negative effects on the cells, especially in the presence of inhibitors. MCD increases JMJD3 gene expression by increasing the gene expression of HIF-1α, which allows for the increased binding of HIF-1α to the *JMJD3* HRE promoter, thus causing the subsequent increase of JMJD3 gene expression[78]. While the 10 nM echinomycin data did not significantly alter *JMJD3* expression in MCD-treated THP-1 macrophages in Figure 5B, this may be because the expression of *JMJD3* in THP-1 macrophages treated with MCD only may have been too low; Figure 5A shows an increase of 5.7-fold in *JMJD3* expression upon MCD treatment. Because the assessment of JMJD3 gene expression was not the core focus of this project, not many repetitions of experiments were conducted to produce numerous valid experiments.

The concentration of 5 nM echinomycin being proposed to inhibit the effect of MCD on *JMJD3* expression originates from a titration of 1-100 nM echinomycin. In this titration that was performed at an earlier time than most of the figures presented in the results section, 10 nM echinomycin reduced the effect of 3 mM MCD during 1-hour co-incubation to near basal levels of *JMJD3* expression. However, this titration was retroactively omitted from the data due to poor RNA quality, deeming it invalid as per Chapter 2.6. Figure 10 presents the only valid experiment from assays using echinomycin, which renders inconclusive results, highlighting the need for further

experimental analysis. However, future experiments must also consider that the change in IL-10 and/or TNF-α outputs may not be induced by similar concentrations of echinomycin used for JMJD3. Therefore, the inclusion of another titration with multiple repetitions demonstrating the change in cytokine and epigenetic characters exposed to echinomycin with/without MCD that yields experimentally valid readings is ideal.

4.3 Macrophagic responses to LPS stimulation

LPS is recognized by macrophages through the TLR4 complex on the plasma membrane[14,79–81]. This complex then triggers the formation of the NF-κB transcription factor complex and the release of inflammatory cytokines such as TNF-α, which is secreted more rapidly than IL-10[80,82]. The secretion of both IL-10 and TNF-α is mediated by TLR4, which was confirmed in the THP-1 macrophages given the consistent, significant increase of both IL-10 and TNF-α outputs in LPS treated groups relative to BSA/RPMI controls.

Cholesterol depletion was hypothesized to increase the expression of *JMJD3* and *JARID1* in a HIF-1α dependent manner. JARID1 was later omitted from quantification because the JARID1 mRNA fold change was not as clear as JMJD3; the focus was shifted to JMJD3 to confirm the effect of MCD on THP-1 macrophages.

Acute cholesterol depletion with 3 and/or 5 mM MCD resulted in varying responses in THP-1 cells, which was the major limitation of this study. To address this discrepancy, the following adjustments were made to the experimental layout:

THP-1 monocyte cultures were started from various vials taken from liquid nitrogen tanks belonging to Dr. Xiaohui Zha and Dr. Alexander Sorisky. However, THP-1 macrophages were generated from monocytes obtained from Dr. Xiaohui Zha's liquid nitrogen tanks due to their better survivability and general health. Healthy monocytes from healthy cultures were cryopreserved for future use, however, all cells originate from older cryopreserved THP-1 monocytes, some of which were dated as old as 2005. Ordering new THP-1 monocytes from ATCC presented a challenge as shipments were heavily delayed due to COVID-19 and was never a possibility.

Various MCD concentrations were tested in MCD + LPS macrophages. Initially, both 3 and 5 mM MCD were tested together, as presented in Figure 7. Because the results in Figure 7 show no difference between 3 and 5 mM MCD, 3 mM was the concentration chosen to elucidate a response using the lowest dose of the drug. However, Figure 7 includes only one replicate and the concentration of MCD was later increased back to 5 mM to test if the IL-10/TNF-α response would change, or at least induce consistent results, in MCD + LPS groups to address the discrepancies in cytokine expression and secretion patterns between experiments.

A range of cDNA and media dilutions were tested for RT-qPCR and ELISA. The concentration of cDNA that was diluted for RT-qPCR was determined empirically: manual dilutions of cDNA were performed based on the outcomes of previous assays. As discussed in detail previously, cDNA samples were diluted to adjust the resulting C_t values within 20-30 amplification cycles. Thus, the relationship

between the control and treatment C_t values could reliably be plotted on a linear scale as fold change is determined by 2^-(treatment-control sample).

Different media dilutions were used in the ELISA assay to remain within the kit sensitivity range, and the resulting cytokine readings were multiplied by the dilution factor to calculate the correct cytokine secretion of MCD +/- LPS +/- induced macrophages. As discussed above, the dilution of media allows the value of cytokine concentration to remain within the assay sensitivity range and therefore be plotted directly onto the standard curve instead of extrapolating their values from the generated standard curve.

Plate size for experiments was changed from 12 to 6-well plates for differentiated THP-1 macrophages. This is a significant troubleshooting step because the cDNA obtained from RNA harvested from 12-well plates would not be enough to correspond to 1 ug/sample, therefore cDNA volume would have to be increased to generate 1 ug cDNA, which would be diluted accordingly during qPCR. However, this relationship to mathematically adjust volume to expected cDNA concentration may have not been linear as the spread of cDNA within the sample may not always be homogenous despite extensive pipetting. Increasing the well size simply increased the RNA yield and allowed for increased quantities of cDNA to be generated without any additional calculations. This way, the possibility that these calculations affected the true IL-10 and TNF-α expression during LPS + MCD would have been mitigated by just increasing the yield of products. Future experiments could potentially include overseeding the THP-1 monocytes in 12 well plates during

the PMA differentiation process to improve RNA yield and quality, in addition to changing plate types.

While each of these optimizations improved the quality of the experimental results, no optimization effort was able to deliver consistent data with each experimentally valid result set. Therefore, it is hypothesized that the origin of these inconsistencies may not be entirely due to manual error before, during or after each experiment. Therefore, future experiments exploring this subject must include:

- Investigating other HIF-1α dependent effectors of H3K27me3 and H3K4me3 to compare the related expression related to JMJD3. Potential candidates of such effectors could be UTX or KDM2, which target H3K27me3 and H3K4me3, respectively[83–85]. Other HIF-1α targets, such as iNOS, could also be utilized as controls of HIF-1α dependency.
- Characterizing other cytokines with similar roles to IL-10 and TNF-α and comparing their behavioral outcomes. Potentially, IL-1β and IL-4 could also be characterized alongside the current cytokines, as discussed further in detail below.
- Increasing the number of housekeeping genes used during RT-qPCR to three, as opposed to having used only one housekeeping gene during this project. The experimental samples could be normalized to the geometric mean of the three controls, resulting in a more robust measurement of gene expression.

- Comparing the results of this project to ATAC-seq and CHIP-seq data of THP-1 macrophages that were exposed to the same treatments as described in Chapter Two: Materials and Methods.
- Testing the above experimental protocols in THP-1 macrophages derived from monocytes newly delivered from the ATCC. Other cell lines and primary macrophages could also be tested to determine the response to cholesterol depletion across different types of multiple human macrophages.

4.4 The effect of echinomycin on LPS-challenged THP-1 macrophages pretreated with MCD.

Echinomycin is a small molecule HIF-1α inhibitor that prevents the mature HIF-1α protein from binding to HRE in the target gene promoters[68]. Given that MCD increased *JMJD3* expression in THP-1 macrophages as shown above, and that JMJD3 requires HIF-1α to induce its transcription[46], it was hypothesized that echinomycin would be able to reduce the effect of MCD on JMJD3 expression.

Echinomycin pretreatment displayed inconclusive effects on cytokine output in MCD-treated cells by inducing different changes in IL-10 and TNF-α within the same experiment. This may have been due to uncharacterized changes in the cells or experimental conditions, reagents and/or laboratory experimental operating procedures. Describing the effect of echinomycin on THP-1 macrophages in this project is not possible because only one experiment using echinomycin, MCD and LPS was deemed experimentally valid. Without proper statistical analyses, such as ANOVA, t-test or even standard deviation calculations, and enough valid replicates,

the effect of echinomycin on IL-10 and TNF-α expression and secretion in LPS-stimulated THP-1 macrophages pretreated with MCD remains to be further investigated.

Two checkpoints were assessed during inhibitor studies:

1. LPS + MCD must increase IL-10 and decrease TNF-α expression/secretion relative to LPS controls. This is what was presented in our proposed model (Figure 3) and is what is described in the literature of cholesterol-depleted macrophages.
2. If the first objective is met, echinomycin can be administered/samples can be analyzed.

To further investigate the role of echinomycin on cytokine secretion, higher concentrations of echinomycin were tested but were not quantified or presented in this thesis due to experimental invalidity, mainly due to poor RNA quality, or because the first objective was not met.

4.5 Limitations of this project

The first step in this study should have been to confirm the effect of MCD by conducting a lipid assay, as initially proposed at the beginning of this project. Because MCD traps cholesterol within its cyclic structure and removes it to the media, MCD treatments could have been validated by comparing cellular cholesterol content before and after MCD use: cellular cholesterol should be lower after successful MCD treatments.

This study assumes consistent cytokine expression throughout pro- and anti-inflammatory cytokines; with IL-10 being representative of immune-modulating genes and TNF-α being representative of pro-inflammatory genes, the degree of which cholesterol affects various pro- and anti-inflammatory genes is not accounted for. The cytokine output is taken as a ratio to normalize for TLR4, but there is no normalization for the degree of influence of cholesterol chelation on these genes given that IL-10 expression and secretion peaks hours after TNF-α[38,86].

This project only uses JMJD3 as the marker for marked changes in the epigenetic landscape. Other H3K27me3 targeting enzymes, such as EZH2, or other representatives for proinflammatory and anti-inflammatory genes should have been utilized, such as IL-1β and IL-6 to be used alongside TNF-α to assess the M1 state in THP-1 macrophages, or IL-4 to support the findings of IL-10 expression and secretion as a marker for the M2 phenotype. The importance of using additional markers of inflammation is exacerbated when JMJD3 was found to influence the expression of 70% of LPS target genes, yet none of these genes were observed to be completely reliant on JMJD3 activity alone[45]. While included in the originally proposed model, studies of *JARID1* expression were discontinued due to the minimal fold change induced by MCD; characterizing *JMJD3* expression with and without MCD first would have given more insight because the fold change in *JMJD3* is starker relative to the changes in *JARID1*, and existing results quantifying *JARID1* expression were omitted from this thesis due to their experimental invalidity as described in Chapter 2.6.

Technical limitations of this project include the lack of utilizing HIF-1α target genes in addition to *JMJD3*, such as *iNOS*, during studies utilizing echinomycin to test inhibitor validity. The resulting RT-qPCR values from all experiments could have been normalized to not just one, but to the mean of three housekeeping genes. In addition to *HPRT1*, *ACTB* (beta-actin) and *RPL37A* (ribosomal protein 37A) are the most stable housekeeping genes for THP-1 cells[87], and therefore could have been used as potential housekeeping genes to utilize to determine the expression of target genes. The RT-qPCR thermal profile was not optimized for each individual primer, as melt curves were used to determine primer performance. Moreover, no standard curve was performed for cDNA dilutions, which would have been a more efficient solution to cDNA dilution factors than empirical dilutions. Future experiments may also include the addition of a control group with MCD alone, and a separate control group for each DMSO concentration instead of incorporating only one DMSO loading control with the highest concentration of echinomycin.

The most significant limitation of this study was the COVID-19 pandemic, where students and staff were under quarantine between March and July 2020 and operated with restrictions while in the laboratory throughout the pandemic. This thesis is short three months of benchside experimentation and learning, which could have otherwise changed the outcome of this project significantly.

Given the COVID-19 pandemic, access to primary human macrophages was also limited. Therefore, studies were conducted in THP-1 macrophages only. As discussed in earlier passages, while THP-1 cells are an established cell line that closely resembles human macrophages *in vitro*, they are immortalized from the

blood of an infant boy with acute monocytic leukemia[54]. The cancerous nature of these cells may have uncharacterized changes at the epigenetic, transcriptional, and translational levels when compared to primary monocyte-derived macrophages from healthy donors.

4.6 Future directions of atherosclerosis disease management

Without intervention, the current projections of the costs of cardiovascular disease are expected to rise to $1.1 trillion annually by 2035 for the U.S.A. alone[88]. Atherosclerosis is a polygenic disorder that can be caused by a poor diet and lifestyle in addition to genetic predispositions. The promotion of a healthy lifestyle with plenty of exercise, a good diet and low stress is paramount for the prevention of atherosclerosis, as well as many other illnesses. However, this lifestyle is often idealized and realistically unattainable due to wide disparities in the accessibility to proper nutrition, healthcare, and safe living conditions. This inaccessibility may be exacerbated by low wages and living in a consumption-oriented, capitalist society[89,90], where McDonald's *is* the American dream[91]. As such, the causes of atherosclerosis are multidisciplinary (Figure 11), therefore the research of its mechanisms and treatments must include an equally broad scope of disease management approaches, from assessing the accessibility of nutritious foods to low and middle-income communities, the growing stress burden of emergencies such as the COVID-19 pandemic and rapid climate change.

Despite the use of statins as the primary alternatives for the treatment of atherosclerosis, atherosclerosis can remain a chronic, benign disease until plaque

rupture[92]. In addition to the use of statins to upregulate hepatic LDLR (in addition to their primary function as HMGCR inhibitors)[7], PCSK9 inhibitors such as alirocumab were described to retain hepatic LDLR presence and lower blood cholesterol more effectively than statins, and improve plaque stability by promoting the thickening of the plaque fibrous cap[93]. Moreover, anti-inflammatory drugs such as canakinumab[94] (an IL-1β targeting monoclonal antibody) were shown to prevent future cardiovascular disorders in at-risk patients, showing the potential of treating atherosclerosis through immunological mechanisms independent of lipid biology.

Repurposing prescription drugs for atherosclerosis treatment has been described in the literature. Metformin, a histone deacetylase (HDAC) activator[95], is an already widely used prescription drug for the primary and secondary treatments of diabetes[96], and studies examining the extended applications of metformin as an anti-ageing[97] or anti-cancer[98] tool are present in the literature. One study[99] showed that metformin was able to reverse conditions associated with atherosclerosis in ApoE-deficient mice after 12 weeks of metformin treatment, such as reversing the increase in LDL, triglyceride, total cholesterol and decrease in HDL that was initially caused by a high-fat diet.

The next step of atherosclerosis therapy includes increased personalized and precision medicine. The development of personalized medicine approaches to atherosclerosis therapy includes a potential application of this project: assessing the epigenetic landscape of at-risk individuals by using the molecular and epigenetic markers described in Figure 3. Current treatment options for atherosclerosis through epigenetic mechanisms include the targeting of histone modifications[47,95]. Mainly,

histone methylation and acetylation are described as targets for atherosclerosis therapy. For example, the deficiency of the histone deacetylase *Hdac9* was shown to give rise to increased cholesterol efflux and immune-modulating, M2-like phenotypes in mouse bone marrow cells[100]. Additionally, H3K27me3 was found to be globally decreased in atherosclerotic plaques[47,95], though there was no change observed in JMJD3 or EZH2 in the arterial tissue of patients with atherosclerosis when compared to healthy volunteers.

To specifically pertain to this project, the role of other H3K27me3 effectors besides JMJD3 could be investigated to study their interactions with JMJD3 and H3K27me3 in the regulation of inflammatory genes under the influence of changing cellular cholesterol concentrations in THP-1 macrophages. For example, the H3K27me3 methyltransferase and catalytic member of PRC2, EZH2, is associated with the transcription of pro-inflammatory genes and regulates *ABCA1* expression[101,102], and deletion of *Ezh2* was correlated with the progression of atherosclerosis in mice[102]. Therefore, *EZH2* expression under MCD and/or echinomycin treatment could have been characterized in THP-1 macrophages specifically in this project.

To complement the development of personalized medicine through the characterization of potential molecular targets, increasing access, and frequency if needed, to genetic testing and counselling is also paramount to effectively establish the knowledge gained from the bench to the bedside, thus improving health equity and the fair management of medical resources.

In conclusion, in addition to the promotion of a healthy diet and lifestyle and increasing access to healthcare through macro- and microsocial mechanisms, understanding the inflammatory background of atherosclerosis is essential to developing precise and personalized therapies. Therefore, characterizing the molecular and epigenetic mechanisms linking macrophage inflammation and cholesterol in atherosclerotic development is a promising candidate for the development of novel biomarkers.

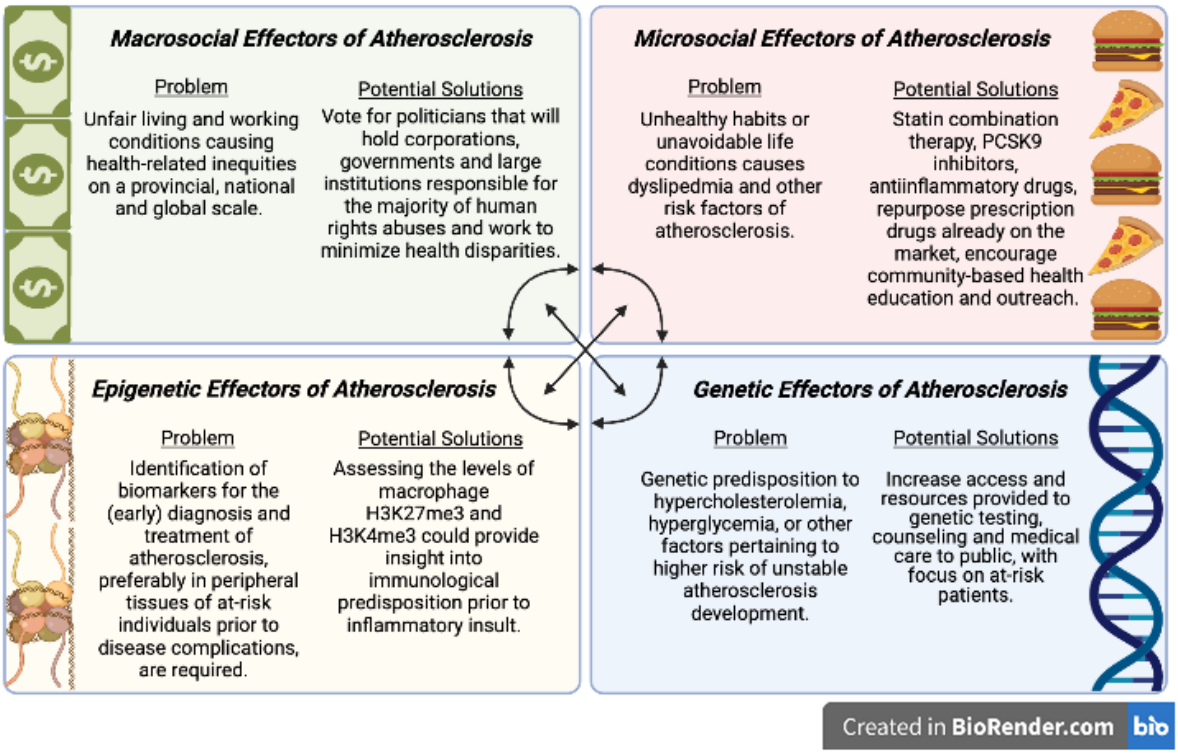

Figure 11. Atherosclerosis: a multifactorial disease.
In this project, we discuss and investigate the influence of cholesterol on macrophage inflammatory behavior, and state that this influence is mediated by epigenetic regulators. However, social, genetic, and epigenetic factors all contribute to the development of atherosclerosis. It is important to note that macro- and micro-social categories refer to the level of challenges presented: food is categorized as a microsocial category due to eating habits, however it can also be categorized as a macrosocial category when referring to food disparity and culinary culture.

Image created with BioRender.com.

CHAPTER FIVE: Conclusion

This work is important to understand the responses of human macrophages to inflammatory stimuli *in vitro* in the presence of low cellular cholesterol and to characterize the changes in the epigenetic intermediary players between cholesterol input and cytokine output upon inflammatory stimulation. Lipid-loaded macrophages contribute heavily to pro-inflammatory, pro-atherosclerotic regions, and addressing the epigenetic mediators of inflammation induced by changes in cellular cholesterol can further the understanding of atherosclerosis.

Herein, the gene expression of the H3K27me3 demethylase JMJD3 is reported to increase in THP-1 macrophages upon 1 hour of MCD pretreatment. However, the resulting IL-10 and TNF-α responses in MCD-pretreated macrophages upon 3 hours of LPS stimulation has been inconsistent throughout this project. In an experiment where MCD + LPS treatment increased IL-10 and decreased TNF-α output relative to LPS treatment alone, echinomycin cotreatment with MCD also resulted in inconsistent cytokine outputs. Therefore, more evidence linking cholesterol and macrophage behavior through epigenetic mechanisms is required.

In summary, the findings of this study are inconclusive and further testing exploring the THP-1 macrophage epigenetic priming and subsequent immune response to changing cellular cholesterol concentrations are required.

References

1. Tarride, J.-E. *et al.* A review of the cost of cardiovascular disease. *Can. J. Cardiol.* **25**, e195–e202 (2009).
2. Epidemiology of Atherosclerosis and the Potential to Reduce the Global Burden of Atherothrombotic Disease. *Circ. Res.*
3. Stamatikos, A. *et al.* Exosome-Mediated Transfer of Anti-miR-33a-5p from Transduced Endothelial Cells Enhances Macrophage and Vascular Smooth Muscle Cell Cholesterol Efflux. *Hum. Gene Ther.* **31**, 219–232 (2020).
4. Luo, Y. *et al.* Macrophagic CD146 promotes foam cell formation and retention during atherosclerosis. *Cell Res.* **27**, 352–372 (2017).
5. Yurdagul, A., Finney, A., Woolard, M. D. & Orr, A. W. The Arterial Microenvironment: The Where and Why of Atherosclerosis. *Biochem. J.* **473**, 1281–1295 (2016).
6. Moore, K. J. & Tabas, I. Macrophages in the Pathogenesis of Atherosclerosis. *Cell* **145**, 341–355 (2011).
7. Istvan, E. Statin inhibition of HMG-CoA reductase: a 3-dimensional view. *Atheroscler. Suppl.* **4**, 3–8 (2003).
8. Should Aspirin Be Used for Primary Prevention in the Post-Statin Era? | NEJM. *N. Engl. J. Med.*
9. Rodriguez, F. *et al.* Association of Statin Adherence With Mortality in Patients With Atherosclerotic Cardiovascular Disease. *JAMA Cardiol.* **4**, 206–213 (2019).

10. Milutinović, A., Šuput, D. & Zorc-Pleskovič, R. Pathogenesis of atherosclerosis in the tunica intima, media, and adventitia of coronary arteries: An updated review. *Bosn. J. Basic Med. Sci.* **20**, 21–30 (2020).
11. Iannuzzo, G. *et al.* Association between causative mutations and response to PCSK9 inhibitor therapy in subjects with familial hypercholesterolemia: A single center real-world study. *Nutr. Metab. Cardiovasc. Dis. NMCD* S0939-4753(21)00543–3 (2021) doi:10.1016/j.numecd.2021.10.025.
12. Mundi, S. *et al.* Endothelial permeability, LDL deposition, and cardiovascular risk factors—a review. *Cardiovasc. Res.* **114**, 35–52 (2017).
13. Badimon, L., Luquero, A., Crespo, J., Peña, E. & Borrell-Pages, M. PCSK9 and LRP5 in macrophage lipid internalization and inflammation. *Cardiovasc. Res.* **117**, 2054–2068 (2021).
14. Nogieć, A., Bzowska, M., Demczuk, A., Varol, C. & Guzik, K. Phenotype and Response to PAMPs of Human Monocyte-Derived Foam Cells Obtained by Long-Term Culture in the Presence of oxLDLs. *Front. Immunol.* **11**, 1592 (2020).
15. Miller, Y. I. *et al.* Oxidation-Specific Epitopes are Danger Associated Molecular Patterns Recognized by Pattern Recognition Receptors of Innate Immunity. *Circ. Res.* **108**, 235–248 (2011).
16. Libby, P. Inflammation in Atherosclerosis—No Longer a Theory. *Clin. Chem.* **67**, 131–142 (2021).
17. Santos, J. C. dos *et al.* Relationship between circulating VCAM-1, ICAM-1, E-selectin and MMP9 and the extent of coronary lesions. *Clinics* **73**, (2018).

18. Park, S. H. Regulation of Macrophage Activation and Differentiation in Atherosclerosis. *J. Lipid Atheroscler.* **10**, 251–267 (2021).
19. Epelman, S., Lavine, K. J. & Randolph, G. J. Origin and Functions of Tissue Macrophages. *Immunity* **41**, 21–35 (2014).
20. Chen, S., Yang, J., Wei, Y. & Wei, X. Epigenetic regulation of macrophages: from homeostasis maintenance to host defense. *Cell. Mol. Immunol.* **17**, 36–49 (2020).
21. RIPK1 Expression Associates With Inflammation in Early Atherosclerosis in Humans and Can Be Therapeutically Silenced to Reduce NF-κB Activation and Atherogenesis in Mice. *Circulation*.
22. Schnack, L. *et al.* Mechanisms of Trained Innate Immunity in oxLDL Primed Human Coronary Smooth Muscle Cells. *Front. Immunol.* **10**, 13 (2019).
23. Rosas-Ballina, M., Guan, X. L., Schmidt, A. & Bumann, D. Classical Activation of Macrophages Leads to Lipid Droplet Formation Without de novo Fatty Acid Synthesis. *Front. Immunol.* **11**, 131 (2020).
24. Sheedy, F. J. *et al.* CD36 coordinates NLRP3 inflammasome activation by facilitating intracellular nucleation of soluble ligands into particulate ligands in sterile inflammation. *Nat. Immunol.* **14**, 812–820 (2013).
25. He, C. *et al.* Effects of β2/aβ2 on oxLDL-induced CD36 activation in THP-1 macrophages. *Life Sci.* **239**, 117000 (2019).
26. Poznyak, A. V. *et al.* Overview of OxLDL and Its Impact on Cardiovascular Health: Focus on Atherosclerosis. *Front. Pharmacol.* **11**, 613780 (2021).

27. Goldstein, J. L. & Brown, M. S. Regulation of the mevalonate pathway. *Nature* **343**, 425–430 (1990).
28. Manjarrez-Reyna, A. N. *et al.* Native Low-Density Lipoproteins Act in Synergy with Lipopolysaccharide to Alter the Balance of Human Monocyte Subsets and Their Ability to Produce IL-1 Beta, CCR2, and CX3CR1 In Vitro and In Vivo: Implications in Atherogenesis. *Biomolecules* **11**, 1169 (2021).
29. Burger, F. *et al.* NLRP3 Inflammasome Activation Controls Vascular Smooth Muscle Cells Phenotypic Switch in Atherosclerosis. *Int. J. Mol. Sci.* **23**, 340 (2021).
30. Ahmadian, M. *et al.* PPARγ signaling and metabolism: the good, the bad and the future. *Nat. Med.* **19**, 557–566 (2013).
31. Englund, M. C. O., Karlsson, A.-L. K., Wiklund, O., Bondjers, G. & Ohlsson, B. G. 25-hydroxycholesterol induces lipopolysaccharide-tolerance and decreases a lipopolysaccharide-induced TNF-α secretion in macrophages. *Atherosclerosis* **158**, 61–71 (2001).
32. Yan, J. & Horng, T. Lipid Metabolism in Regulation of Macrophage Functions. *Trends Cell Biol.* **30**, 979–989 (2020).
33. Poznyak, A. V. *et al.* Renin-Angiotensin System in Pathogenesis of Atherosclerosis and Treatment of CVD. *Int. J. Mol. Sci.* **22**, 6702 (2021).
34. Li, Z. *et al.* Studying the Factors of Human Carotid Atherosclerotic Plaque Rupture, by Calculating Stress/Strain in the Plaque, Based on CEUS Images: A Numerical Study. *Front. Neuroinformatics* **14**, 596340 (2020).

35. Nguyen, M. T. *et al.* Inflammation as a Therapeutic Target in Atherosclerosis. *J. Clin. Med.* **8**, 1109 (2019).
36. Creative Commons — Attribution 4.0 International — CC BY 4.0. https://creativecommons.org/licenses/by/4.0/.
37. MDPI | Open Access Information. https://www.mdpi.com/openaccess.
38. Tedesco, S. *et al.* Convenience versus Biological Significance: Are PMA-Differentiated THP-1 Cells a Reliable Substitute for Blood-Derived Macrophages When Studying in Vitro Polarization? *Front. Pharmacol.* **9**, 71 (2018).
39. Gajanayaka, N. *et al.* TLR-4 Agonist Induces IFN-γ Production Selectively in Proinflammatory Human M1 Macrophages through the PI3K-mTOR– and JNK-MAPK–Activated p70S6K Pathway. *J. Immunol.* **207**, 2310–2324 (2021).
40. Forrester, M. A. *et al.* Similarities and differences in surface receptor expression by THP-1 monocytes and differentiated macrophages polarized using seven different conditioning regimens. *Cell. Immunol.* **332**, 58–76 (2018).
41. Gerrick, K. Y. *et al.* Transcriptional profiling identifies novel regulators of macrophage polarization. *PLOS ONE* **13**, e0208602 (2018).
42. Black, J. C., Van Rechem, C. & Whetstine, J. R. Histone Lysine Methylation Dynamics: Establishment, Regulation, and Biological Impact. *Mol. Cell* **48**, 491–507 (2012).
43. Glass, C. K. & Natoli, G. Molecular control of activation and priming in macrophages. *Nat. Immunol.* **17**, 26–33 (2015).

44. Groh, L. A. *et al.* oxLDL-Induced Trained Immunity Is Dependent on Mitochondrial Metabolic Reprogramming. *Immunometabolism* **3**, e210025 (2021).
45. Francesca De Santa *et al.* Jmjd3 contributes to the control of gene expression in LPS-activated macrophages. *EMBO J.* **28**, 3341–3352 (2009).
46. Lee, H.-Y., Choi, K., Oh, H., Park, Y.-K. & Park, H. HIF-1-Dependent Induction of Jumonji Domain-Containing Protein (JMJD) 3 under Hypoxic Conditions. *Mol. Cells* **37**, 43–50 (2014).
47. Wierda, R. J. *et al.* Global histone H3 lysine 27 triple methylation levels are reduced in vessels with advanced atherosclerotic plaques. *Life Sci.* **129**, 3–9 (2015).
48. Salminen, A., Kaarniranta, K. & Kauppinen, A. Hypoxia-Inducible Histone Lysine Demethylases: Impact on the Aging Process and Age-Related Diseases. *Aging Dis.* **7**, 180–200 (2016).
49. Satoh, T. *et al.* The Jmjd3-Irf4 axis regulates M2 macrophage polarization and host responses against helminth infection. *Nat. Immunol.* **11**, 936–944 (2010).
50. Ma, L., Dong, F., Zaid, M., Kumar, A. & Zha, X. ABCA1 Protein Enhances Toll-like Receptor 4 (TLR4)-stimulated Interleukin-10 (IL-10) Secretion through Protein Kinase A (PKA) Activation*. *J. Biol. Chem.* **287**, 40502–40512 (2012).
51. Rius, J. *et al.* NF-κB links innate immunity to the hypoxic response through transcriptional regulation of HIF-1α. *Nature* **453**, 807–811 (2008).

52. Fitzpatrick, S. F. *et al.* An Intact Canonical NF-κB Pathway Is Required for Inflammatory Gene Expression in Response to Hypoxia. *J. Immunol.* **186**, 1091–1096 (2011).
53. Bullen, J. W. *et al.* Protein kinase A-dependent phosphorylation stimulates the transcriptional activity of hypoxia-inducible factor 1. *Sci. Signal.* **9**, ra56 (2016).
54. Tsuchiya, S. *et al.* Establishment and characterization of a human acute monocytic leukemia cell line (THP-1). *Int. J. Cancer* **26**, 171–176 (1980).
55. Seo, M. *et al.* Statins Activate Human PPARα Promoter and Increase PPARα mRNA Expression and Activation in HepG2 Cells. *PPAR Res.* **2008**, 316306 (2008).
56. Luo, J., Yang, H. & Song, B.-L. Mechanisms and regulation of cholesterol homeostasis. *Nat. Rev. Mol. Cell Biol.* **21**, 225–245 (2020).
57. Human Apolipoprotein A-II Protects Against Diet-Induced Atherosclerosis in Transgenic Rabbits | Arteriosclerosis, Thrombosis, and Vascular Biology. https://www-ahajournals-org.proxy.bib.uottawa.ca/doi/full/10.1161/ATVBAHA.112.300445.
58. Ouimet, M., Barrett, T. J. & Fisher, E. A. HDL and Reverse Cholesterol Transport: Basic Mechanisms and their Roles in Vascular Health and Disease. *Circ. Res.* **124**, 1505–1518 (2019).
59. Yvan-Charvet, L. *et al.* Increased inflammatory gene expression in ABC transporter deficient macrophages: free cholesterol accumulation, increased signaling via Toll-like receptors and neutrophil infiltration of atherosclerotic lesions. *Circulation* **118**, 1837–1847 (2008).

60. Zhu, X. *et al.* Increased Cellular Free Cholesterol in Macrophage-specific Abca1 Knock-out Mice Enhances Pro-inflammatory Response of Macrophages. *J. Biol. Chem.* **283**, 22930–22941 (2008).
61. Horie, T. *et al.* MicroRNA-33 regulates sterol regulatory element-binding protein 1 expression in mice. *Nat. Commun.* **4**, 2883 (2013).
62. miR-33a/b contribute to the regulation of fatty acid metabolism and insulin signaling. *PNAS* https://www.pnas.org/doi/abs/10.1073/pnas.1102281108.
63. Ouimet, M. *et al.* MicroRNA-33–dependent regulation of macrophage metabolism directs immune cell polarization in atherosclerosis. *J. Clin. Invest.* **125**, 4334–4348.
64. Hsu, H.-Y., Nicholson, A. C. & Hajjar, D. P. Inhibition of Macrophage Scavenger Receptor Activity by Tumor Necrosis Factor-α Is Transcriptionally and Post-transcriptionally Regulated. *J. Biol. Chem.* **271**, 7767–7773 (1996).
65. Nekrasova, E. V. *et al.* Regulation of Apolipoprotein A-I Gene Expression in Human Macrophages by Oxidized Low-Density Lipoprotein. *Biochem. Mosc.* **86**, 1201–1213 (2021).
66. Moncan, M. *et al.* Regulation of lipid metabolism by the unfolded protein response. *J. Cell. Mol. Med.* **25**, 1359–1370 (2021).
67. Yang, D. *et al.* Macrophage CGI-58 Attenuates Inflammatory Responsiveness via Promotion of PPARγ Signaling. *Cell. Physiol. Biochem.* **38**, 696–713 (2016).
68. Kong, D. *et al.* Echinomycin, a Small-Molecule Inhibitor of Hypoxia-Inducible Factor-1 DNA-Binding Activity. *Cancer Res.* **65**, 9047–9055 (2005).
69. Loughrey, S. & Matlock, B. Acclaro phenol contaminant ID. 6.

70. real-time-pcr-handbook-life-technologies-update-flr.pdf.
71. Traore, K. *et al.* Signal transduction of phorbol 12-myristate 13-acetate (PMA)-induced growth inhibition of human monocytic leukemia THP-1 cells is reactive oxygen dependent. *Leuk. Res.* **29**, 863–879 (2005).
72. Granucci, F. & Zanoni, I. Role of CD14 in host protection against infections and in metabolism regulation. *Front. Cell. Infect. Microbiol.* **3**, (2013).
73. Starr, T., Bauler, T. J., Malik-Kale, P. & Steele-Mortimer, O. The phorbol 12-myristate-13-acetate differentiation protocol is critical to the interaction of THP-1 macrophages with Salmonella Typhimurium. *PLOS ONE* **13**, e0193601 (2018).
74. Yao, X. *et al.* Leukadherin-1-Mediated Activation of CD11b Inhibits LPS-Induced Pro-inflammatory Response in Macrophages and Protects Mice Against Endotoxic Shock by Blocking LPS-TLR4 Interaction. *Front. Immunol.* **10**, (2019).
75. Daigneault, M., Preston, J. A., Marriott, H. M., Whyte, M. K. B. & Dockrell, D. H. The Identification of Markers of Macrophage Differentiation in PMA-Stimulated THP-1 Cells and Monocyte-Derived Macrophages. *PLOS ONE* **5**, e8668 (2010).
76. Chen, G. *et al.* Methyl-β-cyclodextrin suppresses the monocyte-endothelial adhesion triggered by lipopolysaccharide (LPS) or oxidized low-density lipoprotein (oxLDL). *Pharm. Biol.* **59**, 1036–1044.

77. Rodal, S. K. *et al.* Extraction of Cholesterol with Methyl-β-Cyclodextrin Perturbs Formation of Clathrin-coated Endocytic Vesicles. *Mol. Biol. Cell* **10**, 961–974 (1999).
78. Beyer, S., Kristensen, M. M., Jensen, K. S., Johansen, J. V. & Staller, P. The Histone Demethylases JMJD1A and JMJD2B Are Transcriptional Targets of Hypoxia-inducible Factor HIF. *J. Biol. Chem.* **283**, 36542–36552 (2008).
79. Lu, Y.-C., Yeh, W.-C. & Ohashi, P. S. LPS/TLR4 signal transduction pathway. *Cytokine* **42**, 145–151 (2008).
80. Iyer, S. S., Ghaffari, A. A. & Cheng, G. Lipopolysaccharide-Mediated IL-10 Transcriptional Regulation Requires Sequential Induction of Type I IFNs and IL-27 in Macrophages. *J. Immunol. Baltim. Md 1950* **185**, 6599–6607 (2010).
81. Park, B. S. & Lee, J.-O. Recognition of lipopolysaccharide pattern by TLR4 complexes. *Exp. Mol. Med.* **45**, e66–e66 (2013).
82. Pradines-Figueres, A. & Raetz, C. R. Processing and secretion of tumor necrosis factor alpha in endotoxin-treated Mono Mac 6 cells are dependent on phorbol myristate acetate. *J. Biol. Chem.* **267**, 23261–23268 (1992).
83. Batie, M., Druker, J., D'Ignazio, L. & Rocha, S. KDM2 Family Members are Regulated by HIF-1 in Hypoxia. *Cells* **6**, 8 (2017).
84. Kuang, Y. *et al.* Histone demethylase KDM2B upregulates histone methyltransferase EZH2 expression and contributes to the progression of ovarian cancer in vitro and in vivo. *OncoTargets Ther.* **10**, 3131–3144 (2017).

85. Labbé, R. M., Holowatyj, A. & Yang, Z.-Q. Histone lysine demethylase (KDM) subfamily 4: structures, functions and therapeutic potential. *Am. J. Transl. Res.* **6**, 1–15 (2013).
86. Ernst, O. *et al.* Exclusive Temporal Stimulation of IL-10 Expression in LPS-Stimulated Mouse Macrophages by cAMP Inducers and Type I Interferons. *Front. Immunol.* **10**, 1788 (2019).
87. Maeß, M. B., Sendelbach, S. & Lorkowski, S. Selection of reliable reference genes during THP-1 monocyte differentiation into macrophages. *BMC Mol. Biol.* **11**, 90 (2010).
88. Robinson, J. G. *et al.* Eradicating the Burden of Atherosclerotic Cardiovascular Disease by Lowering Apolipoprotein B Lipoproteins Earlier in Life. *J. Am. Heart Assoc.* **7**, e009778 (2018).
89. Braillon, A. Ending Cardiovascular Diseases, Fast, Effectively, and Cheaply . . . in Capitalist Utopia? *Am. J. Med.* **133**, e323 (2020).
90. Sunderraj, A. *et al.* Associations of Social Vulnerability Index With Pathologic Myocardial Findings at Autopsy. *Front. Cardiovasc. Med.* **8**, 805278 (2021).
91. Mcdowall, C. The Founder: McDonald's – Art of Realising an American Dream. *The Culture Concept Circle* https://www.thecultureconcept.com/the-founder-mcdonalds-art-of-realising-an-american-dream.
92. Li, Y., Shen, S., Ding, S. & Wang, L. Toll-like receptor 2 downregulates the cholesterol efflux by activating the nuclear factor-κB pathway in macrophages and may be a potential therapeutic target for the prevention of atherosclerosis. *Exp. Ther. Med.* **15**, 198–204 (2018).

93. Gao, F. *et al.* Effect of alirocumab on coronary plaque in patients with coronary artery disease assessed by optical coherence tomography. *Lipids Health Dis.* **20**, 106 (2021).

94. Ridker, P. M. *et al.* Antiinflammatory Therapy with Canakinumab for Atherosclerotic Disease. *N. Engl. J. Med.* **377**, 1119–1131 (2017).

95. Napoli, C., Benincasa, G., Schiano, C. & Salvatore, M. Differential epigenetic factors in the prediction of cardiovascular risk in diabetic patients. *Eur. Heart J. - Cardiovasc. Pharmacother.* **6**, 239–247 (2020).

96. Salber, G. J. *et al.* Metformin Use in Practice: Compliance With Guidelines for Patients With Diabetes and Preserved Renal Function. *Clin. Diabetes Publ. Am. Diabetes Assoc.* **35**, 154–161 (2017).

97. Zhao, P. *et al.* Anti-aging pharmacology in cutaneous wound healing: effects of metformin, resveratrol, and rapamycin by local application. *Aging Cell* **16**, 1083–1093 (2017).

98. Wu, D. *et al.* Glucose-regulated phosphorylation of TET2 by AMPK reveals a pathway linking diabetes to cancer. *Nature* **559**, 637–641 (2018).

99. Yan, N. *et al.* Metformin intervention ameliorates AS in ApoE-/- mice through restoring gut dysbiosis and anti-inflammation. *PLoS ONE* **16**, e0254321 (2021).

100. Cao, Q. *et al.* Histone Deacetylase 9 Represses Cholesterol Efflux and Alternatively Activated Macrophages in Atherosclerosis Development. *Arterioscler. Thromb. Vasc. Biol.* **34**, 1871–1879 (2014).

101. Carbone, F. *et al.* Epigenetics in atherosclerosis: key features and therapeutic implications. *Expert Opin. Ther. Targets* **24**, 719–721 (2020).

102. Neele, A. E. *et al.* Myeloid Ezh2 Deficiency Limits Atherosclerosis Development. *Front. Immunol.* **11**, 594603 (2021).

Contributions of Collaborators

I thank Dr. Xiaohui Zha for her supervision and access to her laboratory to conduct this research. Minimal technical assistance was provided by the part-time research technician Xiaoyang (Michelle) Yuan, the postdoctoral fellow Dr. Zeina Salloum and the research technician of the Dr. Alexander Sorisky laboratory, Da Jiang Zhang, as required. All data generated was of my original work and efforts. Feedback, suggestions and guidance with experimental interpretation and planning were provided by Dr. Xiaohui Zha as needed. Dr. Katey Rayner and Dr. Xiaohui Zha reviewed this thesis and approved its final version before submission to the University of Ottawa Faculty of Medicine. Dr. Robin Parks and Dr. Alexander Sorisky provided feedback on experimental results, general knowledge and aims to complete this degree as Thesis Advisory Committee members. Dr. Mireille Ouimet and Dr. Morgan Fullerton served as thesis examiners and members of the thesis defense committee.

Curriculum Vitae

Profile

Outgoing and team-oriented student scientist interested in a career in medical genetics. Recent MSc graduate of the University of Ottawa Faculty of Medicine, Department of Biochemistry with Specialization in Human and Molecular Genetics.

Education

Master of Science, University of Ottawa – *Ottawa/ON, June 2022*

- Area of Study: Biochemistry with specialization in Human and Molecular Genetics.
- Thesis title: “Cholesterol contents in human macrophages regulate inflammatory responses.”
- Thesis supervisor: Dr. Xiaohui Zha.

Honours Bachelor of Science, University of Toronto – *Toronto/ON, June 2019*

- Program of Study: Fundamental Genetics and its Applications (specialist); German (minor).
- Honours project title: “CRISPR-mediated gene correction targeting the *CFTR* locus.”
- Honours project supervisor: Dr. Jim Hu.

Ontario Secondary School Diploma, Appleby College – *Oakville/ON, June 2015*

- Bronze Duke of Edinburgh Award (June 2015)
- Appleby College Model UN Co-Chair and Committee Member (2014-15)
- Secondary Schools United Nations Symposium Delegate (2013 Montreal).

Work Experience

MSc candidate — University of Ottawa, Dr. Xiaohui Zha laboratory
Ottawa/ON, *January 2020 – present*

- Characterized changes in human macrophage behavior (cytokine expression and secretion) caused by cellular cholesterol manipulation for the development of the understanding of human macrophage behavior in atherosclerosis.
- Presented research findings to department and faculty annually at the Biochemistry, Microbiology and Immunology Work-in-Progress presentation, and at the Faculty of Medicine Research Symposium.
- Assisted in the training and orientation of newly recruited graduate students to the laboratory.

Honours Student/Assistant Research Technologist — University of Toronto, Dr. Jim Hu laboratory
Toronto/ON, *September 2018 – August 2019*

- Confirmed viral vector transfection methods in mammalian cell lines for the development of cystic fibrosis gene therapy strategies.
- Created an optimized live-cell imaging protocol to provide a recommendation to management regarding laboratory equipment investments.
- Presented research findings to peers and professors semesterly in a written and oral report.

Residence Life Don — Canadian Campus Communities
Toronto/ON, *September 2017 – April 2018*

- Provided resolutions to client and resident concerns and needs, marketed residence to potential clients and actively participated in residence sales strategies.
- Implemented residence policies and protocols and submitted reports for official records regarding resident and facility upkeep and safety. Updated and regulated residence inventory.
- Planned creative and original initiatives for residence engagement and community outreach.

Clinical Laboratory Intern — VM Medicalpark Hospital
Izmit/Turkey, *May 2016 — June 2016*

- Administered patient samples for clinical analysis and tissue culture, summarized results and reported to physicians for diagnostic purposes.
- Coordinated clinical sample exchange and communicated shipping details to and from external partners.
- Analyzed biological markers from clinical samples using cytology, microbiology laboratory and tissue culture methods in biosafety level 1 and 2 laboratories.
- Shadowed lead physician in the hospital laboratory and observed day-to-day tasks.

Clinic Intern – Ford Motor Company of Europe, Kocaeli Plant
Gölcük/Turkey, *July 2014 — August 2014*

- Updated and maintained confidential plant employee health records online and transitioned medical databases from paper to online systems using MS Excel.
- Organized physical health reports and patient archive libraries for the entire Ford production plant.
- Processed patient intake by administering patient files into the online patient database, and obtained basic medical information (weight, blood pressure) before physician consultation.

- Shadowed physicians during examinations with patients when given patient consent.

Publications and Conferences

Aycan D, Zha X. Cholesterol contents in human macrophages regulate inflammatory responses [unpublished MSc thesis]. University of Ottawa, Ottawa ON. 2022.

Aycan D, Zha X. The human macrophage inflammatory output is regulated by cholesterol depletion. University of Ottawa Faculty of Medicine Virtual Symposium Day, Ottawa ON, September 2021.

Aycan D, Zha X. Cholesterol contents in human macrophages regulate inflammatory responses through epigenetic mechanisms. University of Ottawa Faculty of Medicine Virtual Symposium Day, Ottawa ON, September 2020.

Aycan D, Hu J. CRISPR-mediated gene correction targeting the *CFTR* locus. University of Toronto Honours Course Final Presentation (HMB496), Toronto ON, April 2019.

Aycan D, Hu J. CRISPR-mediated gene correction targeting the *CFTR* locus. Honours Thesis. Human Biology Program, University of Toronto, Toronto ON, April 2019.

Aycan, D. Ancient Egyptian Texts: A Postmodernist Standpoint. St. Michael's College Undergraduate Research Forum. University of Toronto, Toronto ON. February 2017.

Professional Skills

Laboratory skills: RT-qPCR; ELISA; western blotting; viral transfection; molecular cloning; plasmid and primer design; human and mouse macrophage cell culture and maintenance.

Computer skills: R Studio; GraphPad/Prism; MS Excel; MS Office; NCBI BLAST; PyMOL.

Soft skills: Public speaking; Collaboration; Adaptability

Other professional certifications: SixSigma White Belt (in progress); First Aid CPR and AED (St. John's Ambulance).

Languages Spoken

- **English** (native speaker/ fluent)
- **Turkish** (native speaker/ fluent)

- **German** (upper intermediate/ CEFR level B2)
- **French** (lower intermediate/ CEFR level B1)
- **Danish** (beginner/ CEFR level A2)

Extracurricular Activities

Links2Care (*January 2022 – present)*: Phone reassurance volunteer for adults with disabilities and seniors that are experiencing loneliness and isolation in Burlington, ON during COVID-19.

Citizens' Climate Lobby (*August 2021 – present*): Citizens meeting with local and provincial politicians to discuss climate policies for the mitigation of the effects of climate change.

Ottawa Science Innovation Challenge Judge (*February 2021*): Evaluated science fair presentations at the high school level and provided feedback for students regarding their science projects.

Let's Talk Science (*September 2020 – present*): An educational extracurricular that allows K-12 students to meet with student scientists and learn about STEM subjects.

Recognized Study Group Leader (*January 2017 – April 2017*)**:** Peer tutor leader for BIO220: From Genomes to Ecosystems at the University of Toronto. Recognized by the Faculty of Arts and Science Co-Curricular Record.

Residence Council (*October 2016 – April 2017*): Organized events and helped management regarding building administration of Parkside Student Residence in Toronto, ON.

Dean's Cup Representative, House Council (*September 2015 – April 2016*): Organized sports events for residents at Fisher House of St. Michael's College at the University of Toronto.

Student Delegate (*November 2013*): Committee Delegate for the Secondary Schools United Nations Symposium held in Montreal, Canada.

Student Delegate (*May 2012*): Committee Delegate for the Bahçeşehir Colleges Young Diplomats Conference held in Istanbul, Turkey.

Pianist and Guitarist (*January 2011 – present*): Pianist and guitarist that has given live performances at prestigious venues for end-of-year conservatory concerts. Obtained musical training in classical piano and guitar, and widely adaptable to various guitar playing styles such as Spanish and acoustic.